IN THE UNITED STATES PATENT AND TRADEMARK OFFICE

In re Patent Application of

Peter SONDEREGGER

Application No. 09/403,724

Filed: December 20, 1999

For: NEUROTRPYSIN

Group Art Unit: 1646

Examiner: O. Cherneyshev

Confirmation No. 7613

DECLARATION OF DR. PETER SONDEREGGER

I, Peter Sonderegger, hereby declare:

1. I am the inventor of the above-cited patent application.

2. The invention claimed in this application relates to neurotrypsins, and to pharmaceutical compositions containing neurotrypsins.

3. It is my understanding that the Examiner questions the utility of the neurotrypsin molecules claimed in this application. The experiments described below clearly show the biological role of neurotrypsin, the utility of its pharmaceutical modulation, and its production and purification.

Synaptic localization of the neurotrypsin proteins

4. Neurotrypsin is a synaptic protein located in the active zone of the presynaptic terminal (*See* Experiments 1-5, attached). We have demonstrated neurotrypsin to be a protein located at synapses of the central nervous system in both humans and mice. Within the synapse, the neurotrypsin is located at the presynaptic active zone of the presynaptic nerve terminal, which forms the output part of the synapse. By *in situ* hybridization of messenger RNA, (mRNA) we determined the localization of the mRNA at the cellular level in sections through the brains of adult mice. We found that neurotrypsin mRNA is located in neurons in the gray matter of the brain. Because mRNA is generated directly by transcription from an active gene and is not transferred from one cell to the other in eukaryotic organisms, in particular in mammals, it is unequivocally demonstrated that the expression of the neurotrypsin gene occurs in neurons. These experiments are described in detail in Experiment 1, attached.

5. The location of the neurotrypsin protein, which is directly generated by translation of the information encoded by the mRNA, was demonstrated by immunocytochemistry at the

light microscopic level (Experiment 2). Using highly specific antibodies to neurotrypsin, obtained by affinity purification, we found that neurotrypsin protein was abundant in synapse-rich regions in many brain areas. Particularly high concentrations were found in synapse-rich regions of the cerebral cortex, the hippocampus, and the amygdala. However, other synapse-rich regions also exhibited abundant expression of neurotrypsin.

6. To obtain a more detailed localization of neurotrypsin at the synapse, immunocytochemistry was performed at the electron microscopic level with brain tissue preparations from both human and mouse. Using specific, affinity-purified anti-neurotrypsin antibodies, neurotrypsin protein was found in a large number of synapses, which are unequivocally identifiable by their well-known morphology in the neural regions of the central nervous system (For a detailed account see Experiments 3 and 4, attached). At higher magnification, we found that neurotrypsin protein is located in the membrane of the presynaptic terminal, in particular the membrane area lining the synaptic cleft. Based on structural criteria, the most intensive immunostaining for neurotrypsin was found over the synaptic active zones of the presynaptic terminal. Occasionally neurotrypsin immunoreactivity was also observed in vesicles of the presynaptic terminal. It is noteworthy, however, that the majority of the presynaptic vesicles were devoid of neurotrypsin immunoreactivity.

7. As demonstrated in Experiment 4, below the immunocytochemical localization of neurotrypsin in the membrane at the presynaptic active zone was not only found by analysis of mouse brain, but also in human brain, demonstrating that the localization of neurotrypsin is identical in humans and mice.

8. In order to obtain independent evidence for the synaptic localization of neurotrypsin, a biochemical approach was chosen. Synaptosomes were prepared by subcellular fractionation according to a well-established and generally accepted protocol. The proteins of the synaptosomes were analyzed by Western blotting, using specific antibodies against neurotrypsin. We found that neurotrypsin protein was clearly enriched in the synaptosomes compared to mouse brain homogenate. In agreement with the immunocytochemical data, these results localize neurotrypsin at synapses. For an even more detailed localization by this biochemical approach, synaptosomes were further subdivided according to a subcellular fractionation protocol, and synaptic membranes were prepared. In the analysis of the synaptic membranes using the Western Blotting technique, we found that synaptic membranes were further enriched for neurotrypsin when compared to synaptosomes, indicating that synaptic membranes contain the highest concentration of neurotrypsin. These results are in agreement with the observations made in the immunocytochemical analyses.

9. In summary, the results presented in Experiments 1-5 indicate that neurotrypsin is located in the presynaptic terminal, in particular in the presynaptic membrane lining the synaptic cleft at the presynaptic active zone. This localization puts neurotrypsin in a strategic position to control synaptic structure and function.

Neurotrypsin has a biological role as a modulator of synaptic function.

10. Inactivation of neurotrypsin by a truncating deletion in the human neurotrypsin gene results in a severe mental retardation.

11. In collaboration with the laboratory of Dr. Laurence Colleaux, Hôpital Necker-Enfants Malades, Paris (France), we recently reported that neurotrypsin is involved in autosomal recessive mental retardation in humans (Molinari, F. *et al., Science* 298, 1779 – 1781, 2002). By homozygosity mapping in an inbred family with four mentally retarded children, the disease-causing gene was tracked down on chromosome 4q24-q25, were we had previously identified the chromosome localization of the neurotrypsin-encoding gene, PRSS12, by fluorescent in situ hybridization (Kozlov S.V. *et al., Cytogenet Cell Genet.* 84, 107-108, 1999). PCR amplification followed by nucleotide sequence analysis revealed a 4 base-pair deletion in exon 7 of the PRSS12 gene was then found. Exon 7 is encoding for the peptide sequence in the region of the third scavenger receptor cysteine-rich (SRCR) domain. The resulting frameshift in the code leads to the synthesis of a nonsense amino acid sequence before ending in a premature translational stop codon 47 amino acids downstream of the mutation. Thus a truncated, and therefore incomplete, neurotrypsin protein is generated.

12. The truncating deletion in the PRSS12 gene encoding neurotrypsin was found by investigation of an inbred Eastern Algerian family with mentally retarded children (family 1). The parents were first-degree cousins. Four of their eight children (3 girls and 1 boy) were mentally retarded. Cognitive impairment and a low IQ (below 50) were consistent features in the four affected individuals. By means of a genome-wide screen using 400 microsatellite markers, a single region of shared homozygosity on chromosome 4q24-q25 was identified. Further marker typing and haplotype analysis reduced the genetic interval to 18 cM (about 14 Mb) between markers D4S1570 and D4S1575 ($Z_{max} = 3.33$, at $\theta = 0$ at D4S407 locus). This interval contains the PRSS12 gene that encodes the serine protease neurotrypsin (Gschwend, T.P., *et al., Mol. Cell. Neurosci.* 9, 207-219, 1997).

13. Human neurotrypsin is a secreted protein of 875 amino acids, and belongs to the subfamily of trypsin-like serine proteases. It exhibits an unprecedented domain composition consisting of a kringle domain, followed by four scavenger receptor cysteine-rich repeats, and a serine protease domain (Proba K. *et al. Biochim. Biophys. Acta* 1396, 143-147, 1998).

The genomic structure of the human *PRSS12* gene was identified by alignment of the cDNA sequence (Genebank accession number: NM_003619) with the sequence of PAC clone 265B3 (Genebank accession number: AC073025). Thirteen exons were identified and primers were designed for direct sequencing of all coding exons and exon-intron junctions. By this way, homozygosity for a four base-pair deletion in exon 7 of the *PRSS12* gene was detected in one of the affected children. This deletion disrupted an AatII restriction site and resulted in a premature stop codon 147 nucleotides after the mutation. Restriction analyses showed co-segregation of the mutation with the disease in all affected individuals, while both parents were heterozygous. The healthy children that were tested were homozygous for the normal allele. RT-PCR analysis using RNA isolated from a lymphoblastoid cell line derived from an affected child revealed a slightly reduced amount of neurotrypsin transcript in the patient and confirmed the presence of the mutation at the RNA level. This mutation was not found in 200 unrelated control individuals (100 from identical and 100 from different ethnic origins).

14. To estimate the frequency of PRSS12 mutations in patients with severe mental retardation, the PRSS12 coding sequence was screened in 17 inbred non-syndromic mental retardation families and 23 sporadic cases of mentally retarded children. In this study, the deletion mutation (del $ACGT_{1350\text{-}1353}$) was detected in a second family with consanguineous parents and a mentally retarded child. This family (family 2) also originates from Eastern Algeria, but has no known relation to family 1. Restriction analyses in this family confirmed the co-segregation of the mutation with the disease providing new evidence for the pathogenicity of the mutation. Genotyping studies demonstrated that the two families shared a common haplotype across the PRSS12 locus, between D4S406 and D4S1575. Because the two families are unrelated, our data suggest the occurrence of a founder mutation in PRSS12, which may significantly contribute to mental retardation in this population. Careful examination of the affected children from both families revealed a very similar cognitive defect. In both families, the first signs of mental retardation in the affected children were observed at approximately two years of age, after an apparently normal psychomotor development in the first year.

15. The four-nucleotide deletion causes a truncated form of neurotrypsin, which lacks part of the third SRCR domain, the entire fourth SRCR domain, and the entire catalytic domain. Consequently, the generated protein lacks the proteolytic activity of its normal counterpart. The mental retardation phenotype resulting in humans is well compatible with our observations in our ongoing functional studies on neurotrypsin: Neurotrypsin is located in the presynaptic membrane (predominantly the presynaptic active zone) of many, if not all, CNS synapses. Highest expression of neurotrypsin is found in regions involved in memory

and learning, e.g. the cerebral cortex, the hippocampus, and the amygdala. Ongoing investigations in our laboratory indicate a role in hippocampal long-term potentiation, i.e. a generally accepted cellular correlate of memory and learning. The phenotype of the truncating deletion of neurotrypsin in these families is most striking by the loss-of-function in the homozygous individuals, which exhibit a severe mental retardation characterized by an IQ below 50, whereas the heterozygous individuals appear normal (IQ in the normal range). Therefore, the (genetic) inheritance pattern is in full accordance with an autosomal recessive pattern of inheritance. Most typically, the two parents, who are heterozygous for the mutations are healthy.

16. The expression of neurotrypsin in the adult human brain was investigated by immunohistochemistry at the light- and electron-microscopic level (see also Experiment 4). For the specific detection of neurotrypsin, affinity-purified antibodies raised against its proteolytic domain were used. At the light-microscopic level, we found a high density of neurotrypsin-immunoreactive synaptic boutons in the cortical neuropil (Fig. 6A). A more detailed examination at the electron-microscopic level using peroxidase-conjugated secondary antibodies revealed strong neurotrypsin immunoreactivity in the presynaptic nerve ending of cortical synapses, with the most prominent immunoreactivity over the presynaptic membrane lining the synaptic cleft (Fig. 6B). With gold-labeled secondary antibodies, the neurotrypsin immunoreactivity was most prominent in a subpopulation of presynaptic vesicles located adjacent to the presynaptic membrane (Fig. 6C). Thus, neurotrypsin is a presynaptic protein in the adult human CNS.

17. In summary, we have identified a truncating, function-inactivating, four-nucleotide deletion in the gene encoding the synaptic serine protease neurotrypsin as the cause of a severe non-syndromic mental retardation. This provides evidence for the crucial role of neurotrypsin in higher brain function.

Excessive neurotrypsin in neurons of transgenic mice results in enhanced long-term potentiation

Long-Term Potentiation

18. Long-term potentiation (LTP) was discovered by Bliss and Lomo, when they noted that hippocampal synapses are capable of undergoing stable and long-lasting changes in synaptic strength after intensive stimulation (Bliss and Lomo, 1973). They demonstrated that this form of synaptic plasticity has properties strongly suggestive of a role in learning and memory (for a review see Malenka and Nicoll, 1999). For example, the mechanisms of LTP incorporate the sort of specificity, associativity, reversibility, and cooperativity expected of a memory mechanism. Additionally, computer simulations with parallel neuronal networks

inspired by Hebbian-like LTP mechanisms have been shown to process information in a way that is reminiscent of human and animal learning.

20. The question whether LTP is necessary for hippocampal-dependent learning and memory was addressed by many different laboratories with various approaches, including biochemistry, molecular biology, biophysics, neural network theory, and behavioral psychology. Most convincing results were obtained with pharmaceutical perturbations, e.g. by blockage of postsynaptic receptors involved in LTP, but recently also with transgenic animal approaches by which genes involved in LTP were modified or deleted. One of the best-characterized synaptic proteins with a crucial role in LTP is the N-methyl-D-aspartate (NMDA) receptor, a glutamate receptor of the postsynaptic membrane that regulates a calcium channel that is normally blocked by magnesium. To be activated, the NMDA receptor needs two separate events: binding of glutamate (which opens the channel) and postsynaptic depolarization (which removes the magnesium block from the open channel and allows calcium to go through the channel pore). The influx of calcium ions in turn induces a series of biochemical events resulting in the induction and realization of LTP.

21. The first report of unequivocal experimental data indicating a direct relationship between LTP and learning came from the laboratory of R.G.M. Morris at the University of Edinburgh. They found that agents that block the NMDA receptor cause severe deficits in hippocampal LTP and impair hippocampal-dependent spatial learning (Morris et al., 1986). Using pharmacological and transgenic animal technologies, it was subsequently demonstrated that the calmodulin-dependent kinase IIα (CaMKIIα), a signaling molecule strongly expressed in the postsynaptic part of the synapse, was required in its active form, otherwise the mechanisms resulting in the establishment of LTP as well as memory and learning could not be induced. CaMKIIα potentiates synaptic transmission by phosphorylating the NMDA receptors. This in turn increases their conductance and may increase the levels of these receptors in synaptic membranes. Both in mice with null mutations of CaMKIIα and in transgenic mice constitutively overexpressing CaMKIIα LTP was perturbed (Silva et al., 1992). Initial studies with constitutive deletion or expression of CaMKIIα were subsequently complemented with point mutations that generated mutated forms of CaMKIIα, which were active in the absence of calcium (Bach et al., 1995) and, recently, approaches allowing induction of the genetic modification in the adult were added (e.g. Bejar et al., 2002). Altogether, the results of these perturbation experiments clearly demonstrate a role of CaMKIIα in both LTP and learning and memory functions (for recent reviews: Rongo, 2002; Lisman et al., 2002).

22. Most molecular studies aimed at identifying and characterizing synaptic molecules involved in both LTP as well as learning and memory used the hippocampus as the

experimental model. However, the LTP phenomenon is not restricted to the hippocampus, rather it occurs in many brain regions involved in processing higher brain functions. After its discovery in the rabbit hippocampus, LTP has been found in a variety of brain structures and in a number of vertebrate species, including human. For example, LTP has been observed in cat auditory thalamus (Gerren and Weinberger, 1983), rat cerebral cortex (Lee, 1982; Wilhite et al., 1986; Stripling et al., 1988; Laroche et al., 1990), goldfish optic tectum (Lewis and Teyler, 1986), rat olfactory bulb and cortex (Patneau and Stripling, 1992), rat amygdala (Racine et al., 1983, Clugnet and LeDoux, 1990; Maren and Fanselow, 1995), and human hippocampus (Beck et al., 2000).

23. The brain region thought to be most important for learning and memory in the context of higher cognitive functions is the cerebral cortex. In fact, it is widely accepted that the hippocampus is only temporarily involved in learning and memory – eventually, memories are stored in the neocortex (Squire et al., 2001). Other forms of learning and memory, such as fear conditioning, have their most prominent circuitry in the amygdala (Schafe et al., 2001; Goosens and Maren, 2002). Learning of motor skills involves both the cerebral cortex and the cerebellum (Kim and Thompson, 1977; Bao et al., 2002).

24. One of the most impressive studies demonstrating the role of LTP in cortical motor learning has recently been published by Rioult-Pedotti and colleagues (Rioult-Pedotti et al. 1998 and 2000). They trained rats for a task requiring motor skills and found that motor skill learning is accompanied by changes in the strength of connections within the adult rat primary motor cortex (M1). Rats were trained for three or five days in a skilled reaching task with one forelimb, after which slices of motor cortex were examined to determine the effect of training on the strength of horizontal intracortical connections in layer II/III. The amplitude of field potentials in the forelimb region contralateral to the trained limb was significantly increased relative to the opposite "untrained" hemisphere. No differences were seen in the hindlimb region. Moreover, the amount of LTP that could be induced in trained M1 was less than in controls, suggesting that the effect of training was at least partly due to LTP-like mechanisms (Rioult-Pedotti et al. 1998). In a recent follow-up study, they investigated whether learning strengthened these connections through LTP (Rioult-Pedotti et al. 2000). They found that synapses in the trained M1 were near the ceiling of their range of modification, compared with the untrained M1, but the range of synaptic modification was not affected by learning. In the trained M1, LTP was markedly reduced and LTD was enhanced. These results are consistent with the use of LTP to strengthen synapses during learning and represent the first direct evidence that plasticity of intracortical connections is associated with learning a new motor skill.

25. LTP in the cerebral cortex was very recently also demonstrated to be involved in memory consolidation, i.e. a form of plasticity critical for the establishment of permanent memory traces. Making use of the most advanced methodologies for the regional, inducible and reversible genetic modifications in mice, both the NMDA receptor and CaMKII were demonstrated to be required for both LTP and memory consolidation in the cerebral cortex (Shimizu et al., 2000; Frankland et al., 2001; Wang et al., 2003).

26. Since the first publication of LTP by Bliss and Lomo in 1973, the quest for unequivocal evidence for its causal relationship with learning and memory was pursued by numerous neuroscientists with a large variety of methods, in vitro and in vivo. Several critical appraisals of the results obtained and the conclusions drawn from those results have been published over the past years (Martinez and Derrick, 1996; Martin et al., 2000; Martin and Morris, 2002, Matynia et al., 2002; Morris, 2003). They all conclude that there is a wealth of data supporting the notion that synaptic plasticity (in particular LTP) is necessary for learning and memory. For example, in a very careful and rigorous analysis of the experimental facts speaking in favor or against a necessary and sufficient role of LTP in learning and memory, Martinez and Derrick came to the following conclusion: "The rationale for considering LTP a memory mechanism is strong.... After 20 years under scrutiny, LTP remains the best single candidate for the primary cellular process of synaptic change that underlies learning and memory in the vertebrate brain" (Martinez and Derrick, 1996).

27. In summary, there is a wealth of experimental data supporting the conclusion that LTP and memory are intimately connected phenomena. The physiological properties and the cell biological mechanisms of LTP exhibit many other important characteristics of memory mechanisms. Most importantly, LTP has been shown to meet at least three of the four criteria that need to be met in order to be considered as a mechanism that is both necessary and sufficient for the information storage underlying the type of memory mediated by the brain area in which the plasticity is observed:

- changes in synaptic weights are detectable after learning;
- interfering with (or altering) the mechanisms responsible for the induction and expression of synaptic plasticity does indeed interfere (or alter) the rate of learning in a variety of relevant learning paradigms; and
- altering the pattern of synaptic weights after learning also affects the ability of animals to remember a previous learned experience.

28. At present, a rich array of physiological, pharmacological, biochemical, molecular biological, biophysical, genetic, and behavioral data and observations are available and convincingly support and the link between activity-dependent synaptic plasticity (in particular LTP) and memory and learning. Rational scientific reasoning leads to the conclusion that

LTP is the best-characterized and most widely accepted cellular correlate of learning and memory.

Effects of Neurotrypsin on LTP - Evidence from Transgenic Mice. (Experiments 6 and 8)

29. We studied transgenic mice overexpressing neurotrypsin in neurons of the CNS. By stimulating and recording from hippocampal slices, we found a significant enhancement of long-term potentiation in the hippocampal CA1 region of neurotrypsin-overexpressing mice. Mice overexpressing an inactive form of neurotrypsin, lacking catalytic (i.e. proteolytic) activity due to a genetically engineered mutation of the catalytic site serine to an alanine, did not exhibit enhanced long-term potentiation. Likewise, mice expressing an inactive transgene that did not result in production of transgene-derived neurotrypsin, did not exhibit enhanced long-term potentiation. Therefore, the enhanced long-term potentiation in the hippocampus of neurotrypsin-overexpressing mice is due to the catalytic effect derived from excessive neurotrypsin.

30. In summary, neurotrypsin has a concentration-dependent effect on complex synaptic functions. In the total absence of neurotrypsin, cognitive functions are severely impaired, as demonstrated by the occurrence of a severe form of mental retardation in individuals that are homozygous for a defect in the neurotrypsin gene. In contrast, long-term potentiation, a mechanism generally considered as a cellular correlate of synaptic plasticity that underlies learning and memory as well as other higher brain functions, is altered when a higher than normal amount of neurotrypsin is produced in CNS neurons. These observations clearly demonstrate the role of neurotrypsin as a regulator of synaptic functions that is required for memory and learning and other higher brain functions.

The biological role of neurotrypsin as a modulator of synaptic structure: Overexpression of neurotrypsin in neurons of transgenic mice results in a reduced number of synapses in the cerebral cortex and the hippocampus (Experiments 9 – 10)

31. Excessive amounts of neurotrypsin cause a significant change in number and morphology of the synapses in the central nervous system. Evidence for structural changes were found both with electrophysiological and morphological methods. In Experiment 9, a physiological correlate of a reduced neuronal surface area in neurotrypsin-overexpressing mice is reported. Electrical recordings of the capacitance and the change of capacitance after revealed a significantly reduced whole-cell capacitance in hippocampal neurons of neurotrypsin-overexpressing mice. A reduced whole cell capacitance may be due to a reduced surface area of the membrane, if other possible causes can be excluded. Importantly, changed membrane transductance was excluded experimentally as a cause of

the observed change. Therefore, we have investigated the extension and the branching pattern of the neuronal dendrites as well as the size of the neuronal somas. We found no significant deviation of the size at the branching pattern of the neuronal dendrites between neurotrypsin-overexpressing and wild-type mice. Neuronal somas were, if anything, rather enlarged.

32 The observation of a reduced whole-cell capacitance without a reduction of the surface area of the cell soma and the dendrites strongly suggests the reduction in the dendritic spines. The dendritic spines contribute between 50% and 70% to the surface of the neuron and are not included in the measurements of the length and branching pattern of the dendrites. This possibility was evaluated by counting and measuring synapses in neuropil regions and inspecting dendritic spines along dye-filled dendrites (Experiment 10). We found a reduction, both in the number of total synapses per area and in three measurements reflecting synaptic size, namely the area of the presynaptic axon terminal, the area of the postsynaptic spine, and the synaptic length (determined as the length of the apposition of the presynaptic and the postsynaptic membranes. By inspection of the spines along dye-filled dendrites, we found a reduction in the size and the number of spines in the neurotrypsin-overexpressing mice. These measurements are in mutual agreement, because many synapses end on dendritic spines. Therefore, fewer synapses and fewer dendritic spines represent two indicia of the same phenomenon. In addition, reductions in the size of the presynaptic terminal, the postsynaptic spines, and other synaptic parameters, such as synaptic length were found in accordance with smaller, less-well developed spines observed after dye labeling of dendrites.

33. Neurotrypsin clearly qualifies as a protein regulating higher cognitive functions in view of the severe loss of these functions in humans suffering from a genetic defect in the neurotrypsin gene, resulting in the inactivation of the neurotrypsin protein, and contrasting the enhanced long-term potentiation in mice expressing excessive amounts of neurotrypsin in their neurons. It is important to note that human individuals lacking any functional neurotrypsin exhibit normal basic synaptic functions that are required for the neural control of body functions and essential motor and sensory functions. This demonstrates the role of neurotrypsin in the regulation of the plastic and adaptive functions of synapses underlying higher brain functions.

34. In summary, these observations indicate that neurotrypsin is a modulator of synaptic function in brain structures responsible for higher brain functions, such as cognitive functions, learning, and memory. Basic synaptic functions and the formation of synapses during neural development are apparently not affected in the absence of functional neurotrypsin because individuals deficient in active neurotrypsin due to the truncating

deletion in the third SRCR domain had normal neural functions in all other investigated features, including normal motor and vegetative functions.

Neurotrypsin functions as a modulator of a synaptic protein: Neurotrypsin mediates the cleavage of the central nervous system form of agrin (Experiment 12).

35. In order to elucidate the mechanism by which neurotrypsin regulates synaptic structure and function in the central nervous system, we screened for proteins that are cleaved by neurotrypsin. The proteoglycan agrin is present both at the neuromuscular junction (Sanes and Lichtman, 2001) and at synapses of the central nervous system (Smith and Hilgenberg, 2002; Kroger and Schroder, 2002), We found that in the presence of active neurotrypsin, agrin is cleaved. In the presence of neurotrypsin that has been inactivated by replacing the active site serine by an alanine no cleavage of agrin occurs. Thus, clearly, the proteolytic activity of neurotrypsin mediates cleavage of agrin.

36. The form of agrin used in these experiments is the membrane-anchored form. This N-terminally linked form of agrin is predominantly found in the central nervous system and has been reported to play a role in long-term potentiation. Together with the published literature, these results indicated that the enhanced long-term potentiation found in the hippocampus of mice overexpressing neurotrypsin in neurons is due to an excessive cleavage of agrin.

The utility of modulators of the function of the neurotrypsin proteins in the real world.

37. The role of neurotrypsin as a regulator of synaptic structure and function is extensively documented in the Experiments described here. Therefore, neurotrypsin is a target for the development of drugs aimed at modulating synaptic function. Neurotrypsin is indispensable for normal cognitive function of the human brain. Complete inactivity of neurotrypsin in human subjects, due to a truncating deletion in the PRSS12 gene encoding neurotrypsin, causes severe mental retardation. In contrast, excessive levels of neurotrypsin at the synapse cause enhanced long-term potentiation and enhanced neuronal excitability. Therefore, both pharmaceutical drugs that enhance the activity of neurotrypsin and pharmaceutical drugs that reduce the activity of neurotrypsin may be of practical use as regulators of synaptic homeostasis and may counteract cognitive deficits caused by an imbalance of synaptic plasticity.

38. Many of the currently used pharmaceuticals for the treatment of major psychiatric diseases, such as depression and schizophrenia, are agents that modulate synaptic function. Pharmaceuticals that enhance or reduce the function of neurotrypsin are expected

to act in part on the same synaptic functions as drugs commonly used for the treatment of major psychiatric diseases.

Production and purification of the neurotrypsin protein from recombinant protein production systems

39. We have tested a number of eukaryotic protein expression systems with regard to their capacity to produce recombinant neurotrypsin protein for experimental use as a target for drug development (Experiment 12). We demonstrated expression of neurotrypsin in HEK293T-cells and in HEK293EBNA-cells by using transient transfection procedures, we found expression of neurotrypsin in insect cells by using the baculovirus-based expression system, and we found expression of neurotrypsin in myeloma cells by using a stable transfection procedure. The protein produced by these procedures differed, ranging from incompletely processed protein that was retained in the cells to processed protein that was released into the culture supernatant. We have also established a purification procedure for neurotrypsin, consisting of two affinity columns based on specific binding properties of neurotrypsin to heparin and arginine, respectively. These were followed by conventional chromatographic procedures, including ion exchange chromatography and hydrophobic interaction chromatography.

40. I declare further that all statements made herein of my own knowledge are true and that all statements made on information and belief are believed to be true and further that these statements are made with the knowledge that willful false statements and the like so made are punishable by fine or imprisonment or both, under Section 1001 of Title 18 of the United States Code and that such willful false statements may jeopardize the validity of the application or any patent issuing thereon.

Sept 15, 2003
Date

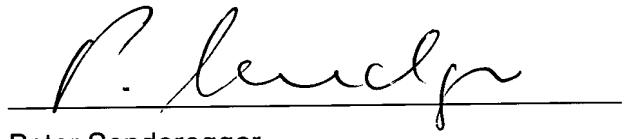
Peter Sonderegger

APPENDIX A

REFERENCES CITED IN DECLARATION

Bach, M.E., Hawkins, R.D., Osman, M., Kandel, E.R., and Mayford, M. (1995). Impairment of spatial but not contextual memory in CaMKII mutant mice with a selective loss of hippocampal LTP in the range of the theta frequency. Cell 81: 905-915.

Bao, S., Chen, L., Kim, J.J., and Thompson, R.F. (2002). Cerebellar cortical inhibition and classical eyeblink conditioning. Proc. Natl. Acad. Sci. USA 99: 1592-1597.

Beck, H., Goussakov, I.V., Lie, A., Helmstaedter, C., Elger, C.E. (2000). Synaptic plasticity in the human dentate gyrus. J. Neurosci. 20: 7080-7086.

Bejar, R., Yasuda, R., Krugers, H., Hood, K. and Mayford, M. (2002). Transgenic calmodulin-dependent protein kinase II activation: dose-dependent effects on synaptic plasticity, learning, and memory. J. Neurosci. 22: 5719-5726.

Bliss, T. and Lomo, T. (1973). Long-lasting potentiation of synaptic transmission in the dentate area of the anaesthetized rabbit following stimulation of the perforant path. J. Physiol. (Lond.) 232: 331-356.

Clugnet, M.C., and LeDoux, J.E. (1990). Synaptic plasticity in fear conditioning circuits: induction of LTP in the lateral nucleus of the amygdala by stimulation of the medial geniculate body. J. Neurosci. 10: 2818-2824.

Frankland, P.W., O'Brien, C., Ohno, M., Kirkwood, A., and Silva, A.J. (2001). α-CaMKII-dependent plasticity in the cortex is required for permanent memory. Nature 411: 309-313.

Gerren, R.A., Weinberger, N.M. (1983). Long-term potentiation in the magnocellular medial geniculate nucleus of the anaesthetized cat. Brain Res. 265: 138-142.

Goosens, K.A. and Maren, S. (2002). Long-term potentiation as a substrate for memory: evidence from studies of amygdaloid plasticity and Pavlovian fear conditioning. Hippocampus 12: 592-599.

Kim, J.J. and Thompson, R.F. (1997). Cerebellar circuits an synaptic mechanisms involved in classical eyeblink conditioning. Trends Neurosci. 20: 177-181.

Kroger, S. and Schroder, J.E., *News Physiol. Sci.* 17: 207 – 212, 2002.

Laroche, S., Jay, T.M., Theirry, A.M. (1990). Long-term potentiation in the prefrontal cortex following stimulation of the hippocampal CA1 subicular region. Neurosci. Lett. 114: 184-190.

Lee, K.S. (1982). Sustained enhancement of evoked potentials following brief, high frequency stimulation of the cerebral cortex in vitro. Brain Res. 239: 617-623.

Lewis, D. and Teyler, T.J. (1986). Long-term potentiation in the goldfish optic tectum in vitro. Brain Res. 375: 246-250.

Lisman, J., Schulman, H., and Cline, H. (2002). The molecular basis of CaMKII function in synaptic and behavioral memory. Nat. Neurosci. 3: 175-190.

Malenka, R.C. and Nicoll, R.A. (1999). Long-term potentiations – A decade of Progress ? Science 285: 1870-1874.

Maren, S. and Fanselow, M.S. (1995). Synaptic plasticity in the basolateral amygdale induced by hippocampal formation stimulation in vitro. J. Neurosci. 15: 7548-7564.

Martin, S.J., Grimwood, P.D., and Morris, R.G.M. (2000). Synaptic plasticity and memory: an evaluation of the hypothesis. Annu. Rev. Neurosci. 23: 649-711.

Martin, S.J. and Morris, R.G.M. (2002). New life in and old idea: the synaptic plasticity and memory hypothesis revisited. Hippocampus 12: 609-636.

Martinez, J.L. and Derrick, B.E. (1996). Long-term potentiation and learning. Annu. Rev. Psychol. 47: 173-203.

Matynia, A., Kushner, S.A., and Silva, A.J. (2002). Genetic approaches to molecular and cellular cognition: a focus on LTP and learning and memory. Annu. Rev. Genet. 36: 687-720.

Morris, R.G.M. (2003). Long-term potentiation and memory. Phil. Trans. R. Soc. Lond. B 358: 643-647.

Morris, R.G.M., Anderson, E., Lynch, G.S., Baudry, M. (1986). Selektive impairment of learning and blockade of long-term potentiation by an N-methyl-D-aspartate receptor antagonist AP5. Nature 319: 774-776.

Patneau, D.K. and Stripling, J.S. (1992). Functional correlates of selective long-term potentiation in the olfactory cortex and ofactory bulb. Brain Res. 585: 219-228.

Racine, R.J., Milgran, N.W., and Hafner, S. (1983). Long-term potentiation phenomena in the rat limbic forebrain. Brain Res. 260: 217-231.

Rioult-Pedotti, M.-S., Friedman, D., Hess, G., and Donoghue, J.P. (1998). Strengthening of horizontal cortical connections following skill learning. Nat. Neurosci. 1: 230-234.

Rioult-Pedotti, M.-S., Friedman, D., and Donoghue, J.P. (2000). Learning-induced LTP in neocortex. Science 290: 533-536.

Rongo, C. (2002). A fresh look at the role of CaMKII in hippocampal synaptic plasticity and memory. BioEssays 24: 223-233.

Sanes, J.R. and Lichtman, J.W. (2001). Induction, assembly, maturation and maintenance of a postsynaptic apparatus. Nat. Rev. Neurosci. 2: 791 – 805.

Schafe, G.E., Nader, K., Blair, H.T., and LeDoux, J.E. (2001). Memory consolidation of Pavlovian fear conditioning: a cellular and molecular perspective. Trends Neurosci. 24: 540-546.

Shimizu, E., Tang, Y.-P., Rampon, C., and Tsien, J.Z. (2000). NMDA receptor-dependent synaptic reinforcement as a crucial process for memory consolidation. Science 290: 1170-1174.

Silva, A.J., Paylor, R., Wehner, J.M. and Tonegawa, S. (1992). Impaired spatial learning in alpha-calcium-calmodulin kinase II mutant mice. Science 257: 206-211.

Smith, M.A. and Hilgenberg, L.G.W. (2002). Agrin in the CNS: a protein in search of function? Neuroreport 13: 1485 – 1495.

Squire, L.R., Clark, R.E., Knowlton, B.J. (2001). Retrograde amnesia. Hippocampus 11: 50-55.

Stripling, J.S., Patneau, D.K., and Gramlich, C.A., (1988). Selective long-term potentiation in the pyriform cortex. Brain Res. 441: 281-291.

Wang, H., Shimizu, E., Tang, Y.-P., Cho, M., Kyin, M., Zuo, W., Robinson, D.A., Alaimo, P.J., Zang, C., Morimoto, H., Zhuo, M., Feng, R., Shokat, K.M., and Tsien, J.Z. (2003). Inducible protein knockout reveals temporal requirement of CaMKII reactivation for memory consolidation in the brain. Proc. Natl. Acad. Sci. USA 100: 4287-4292.

Wilhite, B.L., Teyler, T.J., and Hendricks, C. (1986). Functional relations of the rodent claustral-entorhinal-hippocampal system. Brain Res. 365: 54-60.

APPENDIX B

EXPERIMENT 1: Neurotrypsin messenger RNA is expressed by many neuronal subpopulations of the central nervous system (CNS) and the peripheral nervous system (PNS), (results revealed by *in situ* hybridization).

In order to determine the expression of neurotrypsin messenger RNA (mRNA) in the brain at cellular resolution, *in situ* hybridization was performed as described previously (Schaeren-Wiemers, N. and Gerfin-Moser, A., *Histochemistry* 100: 431–440, 1993). The synthesis of riboprobes was performed by *in vitro* transcription according to standard techniques. To generate sense and antisense riboprobes, full-length cDNA of mouse neurotrypsin (2.3 kb) in the phagemid vector pBluescript (Stratagene) was linearized with restriction enzymes cutting immediately downstream of the cDNA to be transcribed. Using T3 or T7 RNA polymerase and DIG RNA labeling kit (Boeringer), cRNA was synthesized according to the manufacturer's recommendations. cRNA from full length cDNA was subject to partial alkaline hydrolysis in 100mM sodium carbonate pH 10.2 at 60 °C for 20 - 40 min to generate ~300 bp fragments. The riboprobes were then mixed with an equal volume of formamide and stored at -70°C. The size of riboprobes was examined by agarose gel electrophoresis. Riboprobes were used at a concentration of approximately 250 ng/ml.

For *in situ* hybridization, 20 μm cryostat sections were air dried, fixed in 4% paraformaldehyde (in phosphate-buffered saline, pH 7.4) and acetylated with acetic anhydride. After prehybridization in hybridization buffer containing 5xSSC, 50% formamide, 5xDenhardt's solution, 250 μg/ml total yeast RNA, and 500 μg/ml DNA from herring sperm, hybridization was performed at 53°C overnight in hybridization buffer containing the riboprobe. The slides were then washed in graded concentrations of SSC with a high-stringency step of 0.2xSSC/50% formamide at 53°C. Immunological detection of digoxigenin-labeled hybrids was performed using alkaline phosphatase-conjugated anti-digoxigenin antibody and NBT/BCIP. The color reaction was developed in the dark for 12-24 h.

The *in situ* hybridization pattern detected in this way on cryosections from adult mice revealed a strong cellular expression of neurotrypsin mRNA in the gray matter of the central and the peripheral nervous system (Fig. 1). In a coronal section of an adult mouse, highest levels of neurotrypsin mRNA were found in the neocortex, the hippocampal formation, and the amygdala. If the detection sensitivity was adjusted in order to detect intermediate and low level expression, expression of neurotrypsin was also observed in the striatum, the thalamus, the hypothalamus, the cerebellum, the pons, the trigeminal ganglion, and the dorsal root ganglia. No neurotrypsin mRNA was detected in non-neural tissues. Control sections, processed with the sense probe, showed no staining. In conclusion, most, if not all, neurons express neurotrypsin mRNA, yet considerable differences in expression levels were found.

APPENDIX C

EXPERIMENT 2: Neurotrypsin protein is located in the synaptic areas of many regions of the brain (results revealed by immunocytochemistry at the light microscopic level).

To generate the antigen for immunization, the catalytic domain of human neurotrypsin, containing a His-tag at the C-terminus, was produced in *E. coli,* purified on a Ni-NTA column, and refolded. Portions of 50 μg were used for immunization of a goat (primary immunizations in complete Freund's adjuvant and booster injections in incomplete Freund's adjuvant). From the immune serum, IgG was isolated by affinity chromatography on immobilized protein G. Affinity-purified IgG was obtained by affinity chromatography on the immobilized proteolytic domain of neurotrypsin.

The localization of neurotrypsin at the light microscopic level was achieved by means of standard immunocytochemical visualization methods. In brief, adult (6 to 16 week old) C57BL/6 mice of both sexes were deeply anesthetized with metiofane (methoxyflurane, Pitman-Moore Inc.) and perfused through the heart for 15-20 min with fixative composed of 3.5-4% paraformaldehyde (Merck, Switzerland), 0.01-0.02% glutaraldehyde (Merck, Switzerland), and 0.2% picric acid in 0.1 M phosphate buffer, pH 7.4 (PB). The brains were placed into ice-cold PB and sectioned in the coronal plane. Sixty-micrometer-thick vibratome sections were equilibrated in 30% sucrose in PB, rapidly frozen in liquid nitrogen and thawed in PB. The sections were then preincubated in 10% normal rabbit serum (NRbS; Vector Labs, Reactolab, Switzerland) in 0.05 M Tris buffered saline, pH 7.4 (TBS) for 45 min at room temperature.

For immunolabeling, the sections were incubated in primary antibody solution (1:100) in TBS that was supplemented with 2-5% NRbS and 2% bovine serum albumin (BSA, Sigma) for 36-48 hr at 4°C with constant shaking. The sections were then washed (4x20 min in 1% NRbS in TBS) and incubated with biotinylated anti-goat IgG (1:200, Vector Labs) for 12 hr at 4°C followed by 3 hr incubation in an avidin-biotin-peroxidase complex (Elite ABC; 1:100, Vector Labs) at room temperature. Antigenic sites were visualized by incubation in 3,3'-diaminobenzidine (Sigma, Switzerland; 0.05% in TB, pH 7.6) in the presence of 0.0048% H_2O_2. The reaction was stopped by several washes in TB. The sections were mounted on gelatinized slides, air-dried, dehydrated, and coverslipped in Entelan (Merck, Switzerland). The specificity of the immunolabeling was proven by the absence of staining with preimmune serum and when the primary antibodies were omitted.

Applying this procedure of immunoperoxidase staining to tissue sections of the cerebral cortex (Fig. 2), and the hippocampus (Fig. 3A), we found that neurotrypsin was abundant in synapse-rich regions. At higher magnification, a punctate appearance of the immunostaining in the neuropil of the stratum radiatum of the hippocampal CA1 region was found (Fig. 3B). The punctate immunolabeling in a neuropil region is typical for a protein with a synaptic localization. The same pattern of immunolabeling of neurotrypsin was also

observed in the neuropil of other brain regions, including the cerebral cortex, the amygdala, and the caudate putamen.

In conclusion, these results indicate a synaptic localization of neurotrypsin. The synaptic pattern of immunolabeling is found in many regions of the brain. Most prominent immunolabeling for neurotrypsin was found in regions associated with synaptic plasticity.

APPENDIX D

EXPERIMENT 3: Neurotrypsin protein is located in the presynaptic membrane and within the presynaptic active zone of CNS synapses (results revealed by immuno-electronmicroscopy (immuno-EM)).

To reveal the subcellular localization of neurotrypsin in CNS neurons, we used preembedding peroxidase and immunogold immuno-EM. To prepare brain tissue for immuno-EM, adult (6 to 16 week old) C57BL/6 mice of both sexes were deeply anesthetized with metiofane (methoxyflurane, Pitman-Moore Inc., USA) and perfused through the heart for 15-20 min. Mice were first perfused with 0.9% saline for 1 min followed by fixative containing 3.5-4% paraformaldehyde, 0.01-0.02% glutaraldehyde, and 0.2% picric acid made up in 0.1 M phosphate buffer pH 7.4 (PB). Then brains were removed from the skull into cold PB and 70 μm thick coronal sections were cut on a vibratome.

For preembedding immuno-cytochemistry, the sections were cryoprotected in 30% sucrose, quickly frozen in liquid nitrogen, and thawed in PB. After preincubation in 20% normal rabbit serum (NRbS; Vector Labs, USA), sections were incubated in primary antibody diluted in 0.05 mM Tris buffered saline, pH 7.4 (TBS) containing 2% bovine serum albumin (BSA) and 2% NRbS at 4°C for 2 days. For the immunogold method, the sections were incubated overnight in a 1:40 dilution of rabbit anti-goat IgG coupled to 1.4 nm gold (Nanoprobes Inc. Stony Brook, NY), postfixed in 1% glutaraldehyde in phosphate-buffered saline (PBS) followed by silver enhancement of the gold particles with an HQ Silver kit (Nanoprobes Inc). For the peroxidase reaction, the sections were incubated for 4 hr at RT in biotinylated rabbit anti-goat IgG (Vector Labs) diluted 1:200 in TBS containing 1% NRbS, followed by 2 hr incubation in avidin-biotin-peroxidase complex (ABC kit; Vector Labs) diluted 1:100 in TBS. Antigenic sites were revealed using the standard 3,3'-diaminobenzidine tetrahydrochloride histostaining procedure (0.05% DAB and 0.01% H_2O_2 in TB, pH 7.6). The gold-silver and peroxidase-reacted sections were postfixed in 1% osmium tetroxide in PB, stained with 2% uranyl acetate, dehydrated in graded series in ethanol, and flat-embedded on glass slides in Durcupan ACM resin (Fluka) for electron microscopy.

The sections were examined first with a Leica DMR light microscope (LM). Areas of interest were cut from the slide and re-embedded. Serial thin sections were collected on pioloform-coated single-slot copper grids, and examined with a Philips CM100 electron microscope.

Preembedding immuno-EM with peroxidase-labeled antibodies located neurotrypsin on the presynaptic membrane, in particular in the regions of the presynaptic active zone, of synapses located on dendritic spines, dendritic shafts, and on neuronal somas (Fig. 4, A and B). No immunoreactivity was found in dendritic spines. Both asymmetric (excitatory) synapses with round vesicles and thick postsynaptic densities (PSDs) (Type 1 according to Gray, 1959) and symmetric (inhibitory) synapses with pleomorphic vesicles and thin PSDs

(Type 2) exhibited neurotrypsin immunoreactivity. Preembedding immunogold staining of mouse hippocampus confirmed the localization of neurotrypsin in the region of the presynaptic active zone (Fig. 5, A-F). Immunogold-labeling of neurotrypsin was found accumulated within the presynaptic active zone of axon terminals which form asymmetric synapses with dendritic spines (Fig. 5, A and B) and dendritic shafts (Fig. 5, D and E), as well as within active zones of axon terminals which form symmetric synapse with neuronal somata (Fig. 5, C and F).

These results clearly demonstrate that neurotrypsin is a component of the presynaptic membrane in both excitatory and inhibitory synapses of the central nervous system of the mouse.

APPENDIX E

EXPERIMENT 4: Neurotrypsin localization in human brain is identical with neurotrypsin localization in mouse brain (results revealed by immuno-LM and immuno-EM)

The expression of neurotrypsin in the adult human brain was investigated by immunohistochemistry at the light- and electron-microscopic level. The tissue was fixed in 0.1 M sodium phosphate, pH 7.4, containing 4% paraformaldehyde, 0.025% glutaraldehyde, and 0.2% picric acid. Fifty-micrometer thick sections were cut with a vibratome. Incubations of the primary antibody (0.5-2 g IgG/ml) were in 0.05 M Tris-Cl, pH 7.4, supplemented with 2-5% normal rabbit serum and 2-3% bovine serum albumin (Sigma), for 36-48 hr at 4 ^{o}C. For immunoperoxidase localization, the sections were incubated with biotinylated anti-goat IgG (1:200, Vector Labs), followed by incubation with avidin-biotin-peroxidase complex (Elite ABC; 1:100, Vector Labs) and 3,3'-diaminobenzidine (Sigma, Switzerland; 0.05% in Tris-Cl, pH 7.6) in the presence of 0.005% H_2O_2. For immunogold localization, the sections were incubated with the anti-goat IgG conjugated to 1.4 nm gold particles (Nanoprobes) for 3 hr at 21 °C and then subjected to silver intensification with the LI Silver kit (Nanoprobes, USA). Finally, the sections were postfixed in 1% osmium tetroxide and 2% uranyl acetate (Fluka, Switzerland), dehydrated, and flat-embedded in Durcupan ACM (Fluka, Switzerland) for light and electron microscopic examinations.

For the specific detection of neurotrypsin, affinity-purified antibodies raised against its proteolytic domain were used. To generate the antigen for immunization, the catalytic domain of human neurotrypsin, containing a His-tag at the C-terminus, was produced in E. coli, purified on a Ni-NTA column, and refolded. Portions of 50 μg were used for immunization of a goat (primary immunizations in complete Freund's adjuvant and booster injections in incomplete Freund's adjuvant). From the immune serum, IgG was isolated by affinity chromatography on immobilized protein G. Affinity-purified IgG was obtained by affinity chromatography on the immobilized proteolytic domain of neurotrypsin.

At the light-microscopic level we found a high density of neurotrypsin-immunoreactive synaptic boutons in the cortical neuropil (Fig. 6A). A more detailed examination at the electron-microscopic level using peroxidase-conjugated secondary antibodies revealed strong neurotrypsin immunoreactivity in the presynaptic nerve ending of cortical synapses, with the most prominent immunoreactivity over the presynaptic membrane lining the synaptic cleft, in particular in the area of the presynaptic active zone (Fig. 6B). With gold-labeled secondary antibodies, the neurotrypsin immunoreactivity was most prominent within the presynaptic active zone (Fig. 6C). Thus, neurotrypsin is a presynaptic protein in the adult human CNS.

APPENDIX F

EXPERIMENT 5: Neurotrypsin is enriched in purified synaptic membranes (results revealed by subcellular fractionation and immunochemical detection)

To investigate the localization of neurotrypsin by an independent method, the presence of neurotrypsin in so-called synaptosomes and synaptic membranes was determined. Synaptosomes are membrane-bounded structures that are generated by subcellular fractionation. They are composed of the presynaptic terminal, including the presynaptic surface membrane, the synaptic vesicles, the synaptic mitochondria, the presynaptic cytosol, and the presynaptic cytomatrix, as well as the postsynaptic membranes, including the postsynaptic density (PSD) and the cytoplasmic area beneath the postsynaptic membrane. Thus, synaptosomes are essentially isolated synapses. To generate synaptosomes, fresh brain tissue from mice is disrupted by shearing forces, and distinct subcellular organelles and structures are isolated by differential centrifugation. This part was carried out according to the well-established and robust protocol described by Huttner and colleagues (Huttner, W. B. *et al. J. Cell Biol.* 96:1374-1388, 1983). In the second part of the procedure, the preparation and isolation of synaptic membranes out of synaptosomes, we followed the protocol worked out by Jones and Matus (Jones, D.H. and Matus, A. I., *Biochim. Biophys. Acta* 356: 276 - 287, 1974). Because the hypotonic disruption of synaptosomes results in the release of the presynaptic content including the synaptic vesicles, we also added a centrifugation step, in order to obtain a cleaner sample of synaptic vesicles.

The preparatory steps for the isolation of synaptosomes, synaptic membranes, and synaptic vesicles are described in detail below:

1. Preparation of synaptosomes from mouse cerebral cortex

The brains of 20 mice were dissected and put into ice-cold buffered sucrose. The cerebral cortices of 20 brains were pooled and their total weight was determined. The pooled brains were homogenized in 50 ml of buffered sucrose (composed of 320 mM sucrose in 4 mM Hepes-NaOH, pH 7.3) in a glass-Teflon homogenizer (12 strokes, 900 rpm). This process was repeated with another 20 mouse brains. The two homogenates were then pooled and 40 ml of buffered sucrose was added to a final homogenate of approximately 150 ml. The homogenate was centrifuged for 10 min at 800g. The supernatant (S1) was removed and kept on ice; the pellet (P1) was resuspended in 50 ml buffered sucrose. The resuspended P1 was centrifuged again for 10 minutes at 800g. The resulting supernatant S1' was combined with the supernatant S1 and centrifuged for 15 min at 9,200g. The supernatant (S2) was discarded and the pellet (P2) was resuspended by gently vortexing. The resuspension of P2 was done very carefully only with the upper whiter part of the pellet. This upper part of the pellet is distinct from the lower part by a brighter color. The lower (and darker) portion of the pellet consists mainly of mitochondria and was discarded.

The suspension was adjusted to 120 ml of buffered sucrose, and centrifuged for 15 min at 10,500 rpm (10,200g). The supernatant (S2') was removed. The pellet (P2') was resuspended in 13 ml of buffered sucrose (crude synaptosomal fraction), and the suspension was transferred into a glass-Teflon homogenizer. The upper part of the pellet represents the synaptosomes, which were then lysed by adding 117 ml of ice-cold water. The whole suspension was immediately subjected to homogenization (8 strokes, 3,000 rpm). The resulting P2' lysate (L) was poured rapidly into a beaker containing 1 ml of 1 M HEPES-NaOH buffer (pH 7.4). This suspension was stirred for 30 minutes on a magnetic stirrer, while being kept ice-cold. Subsequently the suspension was centrifuged for 20 min at 25,0000 g (16,500 rpm using the SS-34 rotor). The supernatant (LS1, lysate supernatant) was collected for preparing synaptic vesicles. The lysate pellet (LP1) was taken for preparing synaptic membranes. This procedure is based on the method worked out by Huttner and colleagues (Huttner, W. B. *et al. J. Cell Biol.* 96:1374-1388, 1983).

2. Preparation of synaptic plasma membranes (SPM) from the LP1 (plasma membrane enriched) fraction.

The LP1 fraction was resuspended in 4 ml of 7.5 mM HEPES-NaOH, pH 7.2, and 8 ml of 48% (w/w) sucrose (composed of 48% w/w sucrose in 7.5 mM HEPES-NaOH, pH 7.2) was added to obtain a volume of 12 ml and the final concentration of 34% (w/w) sucrose. This cushion of 34% (w/w) sucrose solution was overlayed with a solution of 28.5% sucrose (composed of 28.5% w/w sucrose in 7.5 mM HEPES-NaOH, pH 7.2). On top of this, approximately 2 ml of 10% sucrose solution (composed of 10% w/w sucrose in 7.5 mM HEPES-NaOH, pH 7.2) were overlayed. This step gradient was centrifuged in a 13 ml tube for 110 min in a Beckman SW41 rotor at 22'100 rpm (60'000gav). At the end of this centrifugation, the synaptic membranes form a band at the 28.5% / 34% sucrose interface. This band was collected from the sucrose density gradient by introducing a needle through the side of the centrifuge tube. The synaptic membranes were diluted with 10 ml of 7.5 mM HEPES-NaOH pH 7.2. followed by centrifugation for 30 min in a Beckman SW41 rotor at 29'000 rpm (100'000gmax). The pellet containing the synaptic membranes was resuspended in 1 ml of 7.5 mM HEPES-NaOH pH 7.2.

This procedure was initially developed and published by Jones and Matus (Jones, D.H. and Matus, A. I., *Biochim. Biophys. Acta* 356: 276 - 287, 1974). For a description of the method in form of a protocol see the book chapter by Phelan and Gordon-Weeks (Pheland, P., and Gordon-Weeks, P.R.: Isolation of synaptosomes, growth cones, and their subcellular components. In: *Neurochemistry, a practical approach*, 2nd edition, 1997, Chapter 1, Edited by A.J. Turner and H.S. Bachelard. IRL Press at Oxford University Press).

3. Preparation of synaptic vesicles (SV) from LS1.

The supernatant (LS1) was transferred into 12 10-ml polycarbonate tubes, and centrifuged at 4°C for 2 hr at 50,000 rpm (165,000 g) in a Beckman Ti50 rotor. The resulting supernatant (LS2) was discarded and the pellet (LP2) collected. The pellet (LP2) was resuspended in a total volume of 4 ml of 40 mM sucrose. The suspension was subjected to 10 up-and-down strokes in a glass-Teflon homogenizer at 1,200 rpm. Subsequently, the supernatant was forced 5 times back and forth through a 25-gauge needle attached to a 10-ml syringe. This suspension was then layered on top of a linear continuous gradient (generated in a 38.5-ml polyclear thinwall centrifuge tube from a 800 mM sucrose and a 50 mM sucrose solution), and centrifuged for 5 hr in a Kontron TST 28.38 rotor at 22,500 rpm. Fractions were collected from the sucrose density gradient by introducing a needle through the side of the centrifuge tube. The fractions corresponding to the 200-400 mM sucrose regions (enriched in synaptic vesicles and synapsin I, SG-V) were pooled.

In summary, the preparation of the synaptic membranes consisted in six major steps:
1) homogenization of rat cerebral cortex;
2) differential centrifugation of the homogenate to obtain a crude synaptosomal fraction (P2');
3) hypoosmotic lysis of the synaptosomes to release synaptic vesicles and cytoplasmic components from the synaptic surface membranes (immediately after hypoosmotic lysis, this fraction is termed "crude synaptosomal lysate";
4) differential centrifugation of the crude synaptosomal lysate to obtain a crude synaptic vesicle fraction and a crude synaptic membrane fraction;
5) purification of the synaptic vesicles by continuous sucrose density gradient centrifugation; and
6) purification of the synaptic membrane fraction from the crude synaptic membrane fraction by centrifugation on a sucrose step gradient.
Homogenization and subsequent steps were carried out in low ionic strength media because neurotrypsin was released into the supernatant at moderate and high ionic strength.

The aim of the primary subfractionation of the brain homogenate was to remove small vesicles other than the vesicles contained in nerve endings. Upon osmotic lysis of the P2' fraction, both the small vesicles released into the medium from the synaptosomes and the larger synaptic membranes originating from the surface membranes of the synaptosomes can readily be separated.

To examine the subcellular distribution of neurotrypsin, proteins from subcellular fractions were separated by SDS-polyacrylamide gel electrophoresis, transferred to nitrocellulose, and reacted with an antibody against neurotrypsin (Western blotting). Fig. 7 shows the results of Western blots obtained when equal amounts of protein from the various subcellular fractions were analyzed for the presence of neurotrypsin. It can be seen that, on

Western blots of subcellular fractions, neurotrypsin occurs as two bands with apparent molecular weight of 90 kD and 85 kD. Both bands were recognized by the polyclonal antiserum SZ177 against the proline-rich basic domain of neurotrypsin, and increased following the purification steps. The same enrichment of neurotrypsin immunoreactivity was demonstrated when detected with polyclonal antibody G73 that recognizes the C-terminal protease domain of neurotrypsin. Interestingly, from 90 kD and 85 kD species enriched in the synaptosomes (P2´), only the 85 kD form is found in the synaptic plasma membranes. This could indicate a processing step of neurotrypsin associated with its translocation from intracellular secretory vesicles to the synaptic plasma membrane.

In order to control for the correct tissue fractionation, synaptophysin, a component of the presynaptic vesicles, and NR1 (a subunit of the NMDA-type glutamate receptor), a component of the postsynaptic membrane, were tested on the same fractions. In accordance with the expectations for a successful preparation of synaptic plasma membranes, the synaptic membrane marker NR1 was enriched along the purification process, cumulating in the synaptic membrane (SPM) fraction. Purification proceeded from the brain homogenate (H), via the homogenate supernatant (free of nuclear pellet) (S1), to the crude synaptosomes (P2'), to the crude synaptic plasma membranes (LP1), to the purified synaptic plasma membrane (SPM). Likewise, the synaptic vesicle marker synaptophysin was enriched along the purification process, cumulating in the synaptic vesicle (SV) fraction, i.e. from the brain homogenate (H), via the homogenate supernatant (free of nuclear pellet) (S1), to the crude synaptosomes (P2'), to the crude synaptic vesicles (LP2), to the purified synaptic vesicles (SV). The minor band of synaptophysin in the synaptic membrane fraction is in accordance with the expectations, because approximately 10% of synaptophysin is located in the presynaptic membrane, due to the constant fusion of synaptic vesicles with the presynaptic membrane.

In summary, these results indicate that both neurotrypsin is localized in the synapse, and primarily associated with synaptic plasma membranes. The majority of the synaptic vesicles do not contain neurotrypsin. However, the presence of neurotrypsin in the crude synaptic vesicle fraction (LP2) indicates the presence of neurotrypsin in a minor population of vesicles, comprised in the crude vesicular fraction, but lost in the final purification of the presynaptic vesicles. These results are in accordance with the localization of neurotrypsin in the presynaptic membrane by immuno-EM (Experiments 3 and 4).

APPENDIX G

EXPERIMENT 6: Overexpression of neurotrypsin in neurons using transgenic mice technology.

The overexpression of a gene in a transgenic mouse is used widely to study the function of a protein *in vivo*. For the first series of experiments, neurotrypsin was overexpressed under the control of the promoter of the Thy-1 gene. The Thy-1 gene is expressed in the nervous system of the mouse relatively late (postnatal day 4-10, depending on the location). Therefore, the expression of neurotrypsin under the control of the Thy-1 promoter (Gordon J.W. *et al.*, *Cell* 50: 445-452, 1987) ensures that the earlier developmental stages are not perturbed by the presence of excessive amounts of neurotrypsin. This point is essential. Neurotrypsin is expressed in some regions of the developing nervous system relatively early and, thus, it could play a role in early developmental functions, such as cell migration, axon outgrowth, and synapse formation (Wolfer, D.P. *et al.*, *Molec. Cell. Neurosci.*18: 407-433, 2001). By using a late onset promoter, we intended to prevent perturbations of early stages of neurogenesis in the transgenic animals. However, depending on the aim of an investigation, other promoters may be used as well.

The construct of the first generation transgene was based on an expression vector for Thy-1 in which the translated region of Thy-1 had been substituted by a XhoI linker (Gordon, J.W. *et al.*, *Cell* 50: 445-452, 1987). The full-length cDNA of neurotrypsin was inserted into the Thy-1 expression vector at the XhoI linker site by a blunt-end ligation and the orientation controlled by means of a restriction enzyme digestion and nucleotide sequence analysis. The plasmid is rescued and the fragment to be used for the injection into the pronucleus of fertilized mouse oocytes was cut out by digestion at the two flanking PvuI sites. The injection fragment was separated by electrophoresis in a 1% agarose gel, the band purified with a QIAEXII-kit, and the DNA eluted from the QIAEX particles with injection buffer. The generation of transgenic mice was achieved by pronuclear injection following standard protocol. The litters were screened for the presence of the transgene by polymerase chain reaction (PCR) and Southern blotting.

We found that transgenic mice that overexpressed the neurotrypsin protein in CNS neurons died shortly after birth. To overcome this problem, we generated a second generation of transgenic mice. These mice bore a conditional transgene that was inactive as long as it had not been activated. To generate an inactive, but activatable, transgene, a removable transcriptional stop sequence was introduced before the neurotrypsin-cDNA. This sequence causes transcription to come to a halt. To make the stop sequence removable, an approach based on the Cre/loxP recombination system was chosen (Sauer *B. et al.*, *Proc. Natl. Acad. Sci. (USA)* 85: 5166-5170, 1988). The Cre (Cre-recombinase) protein is encoded by the *Escherichia coli* bacteriophage P1, and efficiently promotes both intra- and intermolecular recombination of DNA in *E. coli*. Recombination occurs at a specific site called

loxP (Hamilton, D.L. and Abremski, K., *J. Mol. Biol.* 178: 481-486, 1984). This characteristic feature of the Cre recombinase allows deletion and insertion of specifically denoted strings of DNA between the loxP sequences. It can be used to generate specific functional mutations *in vivo*. This construct was then inserted between the regulatory subunits of the Thy-1 gene (Chen S. *et al.*, *Cell* 51: 7-19, 1987).

Transfected heterozygous mice with this gene construct were crossed with heterozygous mice carrying Cre-recombinase DNA attached to a cytomegalovirus (CMV) promoter to receive double transgenic (neurotrypsin-overexpressing) mice (see Fig. 8). This promoter is continuously active *in vivo* and the expressed Cre-recombinase promotes recombination at the two loxP sequences. This procedure removes the transcriptional stop sequence from the inactive transgene and allows transcription of the neurotrypsin cDNA. The transgenic mice were genotyped by PCR and Southern blot hybridization. The DNA for the PCR was extracted from the tail of the mice.

The position of the PCR primers was chosen so that the detection of the native murine neurotrypsin gene was prevented. The 3'-primer corresponded to a DNA sequence inside Thy-1.2 and the 5'-primer to a sequence inside the neurotrypsin cDNA. This DNA fragment is unique to the neurotrypsin transgene. The primers for detection of the Cre insert were both equivalent to DNA sequences derived from inside the Cre gene, because Cre usually does not exist in mice. By this procedure, three mouse lines overexpressing the human neurotrypsin and four lines overexpressing the mouse neurotrypsin were raised. The expression of the transgene was verified at the mRNA level by Northern blotting and in situ hybridization and at the protein level by Western blotting. A typical overexpression was in the order of 2- to 3-fold.

In order to control for the dependence of the neurotrypsin-mediated alterations on the catalytic function of neurotrypsin, transgenic mice overexpressing an inactive form of neurotrypsin under the same (Thy-1) promoter were generated. Inactive neurotrypsin can readily be generated by mutating the essential active site serine 711 to an alanine. Because in all serine proteases, the active site serine is involved in a covalent intermediate of the proteolytic reaction, its mutation results in a complete loss of catalytic function. The transgenic mice overexpressing the inactive form of neurotrypsin were healthy and did not exhibit any abnormalities.

By the same method, transgenic animals expressing full-length neurotrypsin, as well as other truncated forms of neurotrypsin or mutated forms of neurotrypsin (point mutations or deletion mutations) may be generated. Instead of the Thy-1 promoter, other promoters may be used, including promoters driving transgene expression in particular subpopulations of neurons, such as the promoter of the Purkinje cell-specific L7 protein or the promoter of the

limbic system-specific protease neuropsin. Alternatively, transgene expression may be put under the control of inducible promoters.

APPENDIX H

EXPERIMENT 7: Increased levels of neurotrypsin in CNS neurons result in enhanced long-term potentiation.

Long-term potentiation (LTP) is due to an increase in synaptic efficacy after an induction paradigm. It is considered a cellular correlate of memory and learning. We induced and measured LTP in the CA1 region of hippocampal slices. An illustration of the position of the electrodes for stimulation and recording is given in Fig. 9. In essence, LTP in other CNS regions, such as the neocortex or the amygdala could also be measured. We restricted our investigation to the hippocampus, since LTP in this area is well-defined and –understood, and accessible to extracellular recordings of field potentials (fEPSPs).

Hippocampal slices were prepared from 17 to 32 day old neurotrypsin-overexpressing and wildtype mice, which were sacrificed by decapitation using a guillotine. The methods for killing and tissue preparation had been approved by the local veterinary authorities and the animal ethics committee. The brains were quickly removed and cooled in ice-cold artificial cerebrospinal fluid (ACSF), which was constantly aerated with 5% CO_2 and 95% O_2 (oxycarbon). Both hemispheres were glued on the cut surfaces with cyanoacrylic glue (Loctile 406, Koenig AG, Dietlikon, Switzerland) onto a horizontal stage of a tissue slicer (Vibratome® 1000, TPI, Evergreen, Missouri, USA) and parasagittal slices cut at a thickness of 300 – 400 µm in ice-cold ACSF. The tissue other than the hippocampus and neocortex was removed from the slices, which were then incubated for 1 hr at 34°C and stored at room temperature for later use.

One of the slices was then transferred to an interface chamber (Haas, H.L. *et al.*, *J. Neurosci. Methods* 1: 323-325, 1979) and laid out on lens cleaning tissue (Whatman International Ltd, Maidstone, England). Recordings commenced 20 minutes later at 35 ± 1°C in the humidified chamber gassed with oxycarbon. fEPSPs were evoked in the Schaffer collaterals using bipolar twisted pair electrodes made from insulated 25 µm diameter tungsten wire (Goodfellow, Huntingdon, England) connected to a Isolator-11 constant-current stimulator (Axon Instruments, Union City, USA). Stimulus currents were adjusted to evoke a fEPSP of about one third of the maximal slope and were typically < 100 µA at 20 – 50 µs duration. The fEPSPs were recorded with patch-electrodes pulled from borosilicate glass (2 mm OD, 1 mm ID, Hilgenberg, Malsfeld, Germany) on a P97 puller (Sutter, Novato, USA) to a resistance of 1 – 2 M when filled with 2 M NaCl using an Axoclamp 2B amplifier (Axon Instruments, Union City, USA). Recordings were amplified 10^4 times after a sample-and-hold step, filtered at 10 kHz using an 8-pole Bessel filter (Design JCSMR, ANU, Australia), and digitized at 20 kHz using a TL-1 interface running PClamp 6 software (Axon Instruments, Union City, USA) on a Pentium II computer.

fEPSPs were evoked in the Schaffer collaterals at 0.03 Hz. CA3 was routinely cut off. Long-term potentiation was induced after a control period of 30 minutes with a "saturating"

paradigm consisting of 4 bursts of tetani at 100 Hz for 1 s separated by 20 s. The fEPSP was monitored for at least 2 hr after induction.

Data were transferred to a Macintosh (Apple computer), and analyzed using custom-made software written for IGOR Pro 4.0 (Wavemetrics, Lake Oswego, USA). The slope of the EPSP was measured at the steepest part, typically within the middle third of the voltage deflection (Moser, E.I. *et al.*, *Science* 259:1324-1326, 1993). The slope was estimated by fitting a line to the data points within this interval of 0.3 – 1.2 ms. Slopes were then normalized to control values and expressed as a percentage increase where 0 represents no change.

Data from different experiments were pooled according to the genetic make-up of the animals into either the wildtype or neurotrypsin-overexpressing group. The average and standard deviation time courses were calculated for the two groups. Significance ($p < 0.05$) was assessed using Student *t*-test.

22 fEPSP experiments with hippocampal slices from 12 wild-type litter mates and 31 with slices from 16 neurotrypsin-overexpressing mice were obtained. Two examples of typical experiments are shown from a wild-type (Fig. 10, A-C) and neurotrypsin-overexpressing (Fig. 10, D-E) mouse. In A and D, the time courses of the average fEPSPs are illustrated above the corresponding recording periods; the dotted lines indicate the recording during control conditions. Each dot in the two time courses represents the slope of the fEPSPs recorded every 30 seconds. In B and E, the absolute values of the slope are given, and in C and F, the same values are normalized to control values.

Figures 10 C and F show the control period, during which there was a slight but not significant run-up of the control response, which was somewhat stronger in slices of neurotrypsin-overexpressing mice. LTP was induced at time zero with the 3 distinct phases associated with LTP: first, the induction phase. It coincides with the time of the tetani and is not illustrated, because no sensible value for the EPSP slope can be measured. Second, LTP expression is marked by an immediate increase in fEPSP slope to a value of about 100% after which, as shown in Fig. 10E, it decays (post-tetanic potentiation, PTP) and rebounds to larger values afterwards. The neurotrypsin-overexpressing mice showed a significant and persistent increase in slope during the first hr after PTP had ceased. Third, maintenance of LTP was expressed during the whole time of recording but got smaller with time, more so in the wild-type littermates than in the neurotrypsin-overexpressing mice. Two normalized average time courses (wildtype and neurotrypsin-overexpressing) were calculated from all valid experiments, and are illustrated in Fig. 11. It shows a greater degree of LTP in the neurotrypsin-overexpressing than in the wild-type mice. Significance based on a *t*-test is indicated by a dot above the appropriate point in time. The increase in LTP at two hr of recording was 122 ± 20% and 83 ± 12% for neurotrypsin-overexpressing and wildtype

mice, respectively. This result indicates that in transgenic animals, synaptic efficacy is increased by 68 ± 15% compared with wild-type littermates.

In the present study, synaptic efficacy at the CA3-CA1 synapses in acute slices of hippocampus was assessed using an electrophysiological assay (change in fEPSP). The main finding is, that after a saturating induction paradigm (Baranes, D. *et al.*, *Neuron* 21:813-825, 1998), LTP is significantly increased in neurotrypsin-overexpressing mice when compared with the wild-type litter mates (122 ± 20 vs. 83 ± 12%). The amount of LTP in wild-type mice, with the genetic background of C57BL/6J inbred mice, is consistent with results obtained in experiments characterizing LTP in different strains of inbred mice (Nguyen, P.V. *et al.*, *J. Neurophysiol* 84: 2484, 2000; Nguyen, P.V. *et al.*, J. *Neurosci.* 20: 6077-6086, 2000). This characteristic of neurotrypsin-overexpressing mice is indicative that, indeed, the action of neurotrypsin is at the synapse. These results are also in line with other studies, in which extracellular proteases were implicated in increased LTP (Baranes, D. *et al.*, *Neuron* 21: 813-825, 1998; Madani, R. *et al.*, *EMBO J.* 3007-3012, 1999).

APPENDIX I

EXPERIMENT 8: Increased levels of neurotrypsin in CNS neurons result in reduced cell capacitance in postsynaptic targets (results revealed by electrophysiological recordings).

When evoking fEPSPs, reverberating activity could be observed in hippocampal slices of neurotrypsin-overexpressing mice at much lower stimulus intensities than in slices of control litter mates: Multiple negative-positive going voltage deflections were observed, particularly after induction of LTP, i.e. after an increase in synaptic efficacy. As shown in Fig. 12, the mean fEPSP traces from a hippocampal slice of a neurotrypsin-overexpressing mouse exhibited reverberations after induction of LTP, a noticeable difference compared to control conditions where there was a less complex response. These reverberations persisted even if CA3 was cut off, and therefore must have been produced in CA1/entorhinal cortex alone. This observation led us to investigate changes in excitability at the single cell level.

Whole-cell patch clamp recordings of CA1 pyramidal cells were done in a submerged chamber with hippocampal slices prepared the same way as described in the previous example. Individual neurons were visualized with an Axioscope microscope (2F, Zeiss, Jena, Germany) fit with differential interference contrast optics using infrared illumination (Stuart, G.J. *et al.*, *Pflügers Archives* 423: 511-518, 1993). The chamber contained ACSF oxygenated by oxycarbon as superfusate (2 ml/min). The chamber was maintained at 35-36°C, which is near physiological temperature. Patch-pipettes (3 – 5 MΩ) were pulled on a P97 puller (Sutter, Novato, USA) and filled with (in mM) 115 K-gluconate, 20 KCl, 10 HEPES, 10 phosphocreatine, 4 ATP-Mg, 0.3 GTP and 13.4 biocytin titrated to pH 7.2 with KOH. Biocytin was used as a marker for subsequent histological processing (see also next experiment).

We obtained basic electrophysiological properties of the action potential (AP), input resistance (R_i) and whole-cell capacitance (C_m) of the cell recorded. To determine height, width at half maximal amplitude (half width) and threshold current of action potentials, short current steps (5 ms) were injected into the cell soma and the resultant voltage deflection was measured. The current was increased in steps of 10 pA and the current, which produced APs 50% of the time, was defined as the threshold current. The membrane potential at which a regenerative action potential was initiated was also measured.

The results are summarized in Table 1. The resting potential (V_m) was measured when breaking into the CA1 pyramidal cells, which were chosen according to their appearance on the TV monitor. On average, V_m was –69 ± 1 in transgenic and –67 ± 1 mV for wild-type animals; both values were not significantly different. The following parameters associated with action potentials were also not different: half width and voltage threshold. However, action potential height (105 ± 2 versus 110 ± 2 mV; $p = 0.05$) and threshold current (-0.40 ± 0.04 versus –0.29 ± 0.02 nA; $p = 0.005$) differed significantly, indicating that a

smaller current can produce action potentials in transgenic than in wild-type mice. The increased height might suggest that the charging of the membrane is faster in transgenic animals than in wild-type mice and thereby producing a slightly bigger action potential (due to shorter inactivation time).

Table 1 Comparison of the basic electrophysiological properties of the pyramidal cells of the hippocampal CA1 region of control and neurotrypsin-overexpressing (DTG) mice

	Control	DTG	P
AP height [mV]	105 ± 2 (n = 21)	110 ± 2 (n = 29)	0.05
AP half width [ms]	1.0 ± 0.1 (n = 21)	1.1 ± 0.1 (n = 29)	0.5
AP threshold voltage [mV]	-50 ± 1 (n = 21)	-50 ± 0.1 (n = 29)	0.25
AP threshold current [nA]	-0.40 ± 0.04 (n = 21)	-0.29 ± 0.02 (n = 29)	0.005
R_i [MΩ]	150 ± 11 (n = 20)	147 ± 7 (n = 26)	1.0
τ_m	24.2 ± 2.0 (n = 20)	18.1 ± 1.4 (n = 26)	0.0005
C_W [pF]	176.1 ± 17.7 (n = 20)	125.8 ± 9.5 (n = 26)	0.0005
V_m [mV]	-69 ± 1 (n = 21)	-67 ± 1 (n = 29)	0.75

The membrane resting potential was measured at the patch pipette at the beginning of the next series of measurement. The membrane voltage response ΔV_m to multiple current steps to the cells ranging from 0.01 nA to 0.05 nA in increments of 0.01 nA and 0.3 ms duration was measured and displayed with respect to time. One example of such a voltage trace is shown in Fig. 13. The following properties of the CA1 pyramidal cells were determined from those measurements: The membrane time constant τ_m was read at the 63% value of the maximum voltage change ΔV_m. The input resistance R_i was estimated by applying the Ohm's law. The resultant membrane voltage was displayed versus the input current and the R_i calculated from the slope $\Delta V_m/\Delta I_i$ in the graph.

To investigate the charging characteristics of the cells, sub-threshold current injections were used to determine the apparent time constant (τ_m) of these cells. An example of such a voltage deflection due to a hyperpolarizing current pulse of –30 pA is shown in Fig. 13 of a wild-type and a transgenic animal. The apparent time constant (τ_m = Δt at 63% ΔV_{max}) is shorter in neurotrypsin-overexpressing animals than in wild-type littermates (18.1 ± 1.4

versus 24.2 ± 2.0 ms, respectively; $p < 0.0005$). At the same time, R_i was not different in both animal groups. Since τ_m is roughly the product of C_m and R_i, and R_i is not different in the two groups, we conclude that C_m must be the cause for the difference. Indeed, the value is 176 ± 18 versus 126 ± 10 pF at a level of significance of $p < 0.0005$. This value supports the above-mentioned increase in action potential height and indicates that the effective membrane area is smaller in neurotrypsin-overexpressing than in wild-type mice.

A lack of significance of the voltage threshold indicates that, at large, the sodium current is the same for both groups. A reduced current threshold together with a slightly increased AP size might be part of the change in excitability observed as reverberating activity. The underlying mechanism is due to a reduced cell surface. It was the aim of the work presented in the next sections (Experiments 9 and 10) to get insight into where the surface area in transgenic animals is reduced.

APPENDIX J

EXPERIMENT 9: Increased neurotrypsin in CNS neurons does not result in reduced number of dendritic arborizations (results obtained by quantitative morphology).

To determine the morphological correlate of the reduced cellular surface area indicated by a reduced C_m, the neurons used for whole-cell recordings were filled with biocytin and stained using the avidin-biotin-peroxidase reaction. After recording, each slice was flattened between two pieces of Millipore filter paper and fixed for 2-3 hours at room temperature in 1% glutaraldehyde, 2% paraformaldehyde and 0.2% picric acid in 0.1 M phosphate buffer (PB), pH 7.4. After fixation, the slice was stored in 0.5% paraformaldehyde in PB at 4°C.

The histological procedure used is similar to the one described earlier (Horikawa, K & Armstrong, W.E., *J. Neurosci. Methods* 25: 1-11, 1988; Kawaguchi, Y. *et al.*, *J. Neurophysiol.* 62: 1052-1068, 1989). After several washes in PB, the slices were treated with 2% H_2O_2 for 15 min. The slices were then pre-incubated in 20% normal goat serum in 0.05 M Tris buffered saline (pH 7.4) containing 0.5% Triton X-100 (TBST) for 30 min at room temperature and subjected to overnight incubation in Vectastain Elite ABC (avidin-biotin-peroxidase) reagent (1:100; Vector Labs, Geneva, Switzerland) in TBST at 4°C. Following five 15 min washes in TBST and Tris buffer (TB, pH 7.6), biocytin containing cells were visualized by incubation in 3,3'-diaminobenzidine (0.05% in TB) in the presence of 0.0048% H_2O_2. The reaction was stopped by several washes in TB. Sections were mounted on slides and coverslipped in Moviol (Hoechst, Frankfurt, Germany).

The neurons were reconstructed three-dimensionally using a Neuron Tracing System (NTS), version 5.1 (Eutectic Electronics Inc., Jersey Court, USA). The neurons in the processed slices were tracked with a microscope (Optiphot-2, Nikon, Tokyo 100, Japan) using a 100x oil immersion objective by entering the 3D coordinates of the stage (NTS Mark 4 Stage) and the diameter measured at this point directly to a PC. The stage and the focus of the system were driven by stepper motors, where the minimum step size for the stage was 0.1μm and for the focus 1μm. The minimum diameter adjustable was 0.1 μm. Not considered were the dendritic spines and local swellings in the axons.

The statistical parameters of a cell were computed from the spatial data by using the NTS software. The estimated error of a single point was ± 2 μm with a bigger error in the focusing axis. Two examples are shown in Fig. 14. They have been randomly chosen and differences between them are not representative for the average data. The scale bar represents 100 μm.

The reconstructions were used to calculate the total dendritic length, total cell volume, total membrane surface area, maximal branching order, mean dendritic segment length, average number of dendritic segments per cell, mean soma area and average soma diameter. The total dendritic length corresponds to the length of all dendritic segments with

their branches. The total cell volume and the total membrane surface area are the sum of the volumes and membrane areas of the soma and the dendritic trees without spines. A dendritic segment was defined as the section of a dendrite between its base at the soma and the first branching point, the section between two branching points or the section between the last branching point and the end of the dendrite. The soma area was estimated from the outline marking the soma.

The results are based on reconstructions of neurons of 11 neurotrypsin-overexpressing and eight wildtype mice. The means of the two groups were calculated together with the standard errors of the mean and displayed in Fig. 15. The data illustrated revealed no significant differences between the control and the neurotrypsin-overexpressing group in spatial parameters (*t*-test) except for soma diameter and area, which were slightly bigger in the neurotrypsin-overexpressing mice.

These results indicate that there is no systematic difference between transgenic and wildtype animals if spines are not taken into account. This points towards a scenario, where the loss of membrane area is confined to dendritic spines, since a very substantial proportion of the dendritic surface area is due to the spines (Cauller L. and Connors, B.W., Functions of very distal dendrites: Experimental and computational studies of layer I synapses on neocortical pyramidal cells. In *Single neuron computation*. ed. McKenna, T., Davis, J. & Zornetzer, S. F., pp. 199-229. Academic Press, Inc., San Diego, CA 92101). In fact, the slightly larger somatic diameter and surface area should have resulted in a bigger C_m, which we did not see, indicating that, indeed, most of the surface lost is within the spines. Since the measurements of C_m and the reconstructions were from the same cells, we are confident that the estimates of surface area are not compromised by slicing artifacts. Since the spines are the loci where synapses form, and since these seem to be reduced in size and/or number, the effect of neurotrypsin is indeed at the synapse, resulting in this case in (partial) removal of the postsynaptic part of the synapse.

APPENDIX K

EXPERIMENT 10: Increased levels of neurotrypsin in CNS neurons result in reduced number and size of synapses (results revealed by quantitative morphology)

In this experiment, we attempted to quantify the number of synapses per volume of tissue of a synapse-rich region, and to measure the size parameters of the synapses. Parameters measured included the area of the presynaptic axon terminals, the area of the postsynaptic spines, and the length of the synapses (as measured by the length of the apposition of the pre- and postsynaptic membrane). Two independent lines of neurotrypsin-overexpressing mice (Nt491/cre and Nt494/cre) and several lines of control mice (wildtype mice, CMV-Cre mice, and the transgenic parental lines bearing the inactive neurotrypsin transgene (Nt491-inact.Nt and Nt494-inact.Nt) were investigated.

The mice were deeply anesthetized at the age of 28 days with metiofane (Schering-Plough, USA) and perfused through the heart with 0.9% sodium chloride followed by fixative consisting of 2% paraformaldehyde, and 1% glutaraldehyde in 0.1 M phosphate buffer pH 7.4 (PB). The brains were removed from the skull and sectioned into 100 μm-thick serial sections with a vibratome. The sections were postfixed in 1% osmium tetroxide in PB, treated with 2% uranyl acetate, dehydrated in ethanol and propylene oxide and embedded in Durcupan ACM resin (Fluka). For electron microscopic analysis strips of sections containing the CA1 region of the hippocampus at the anteriocaudal level Bregma –2 mm and mediolaterally 1.5 mm were ultrasectioned. An illustration of the EM images obtained is given in Fig. 16.

The synaptic sampling procedure consisted of 15 to 23 EM samples of the neuropil of the stratum radiatum of the hippocampal CA1 region from three noncontiguous areas with at least 50 μm distance between each other an initial magnification of 27,500-fold. The electron micrographs were printed at a final magnification of 80,000-fold which represented 90 to 135 μm^2 of tissue. A synapse was defined as two apposed thickened membranes of a presynaptic and postsynaptic profile, with the presynaptic profile containing at least three synaptic vesicles in close association with the differentiated membranes. The synapses were classified into axodendritic and axospinous synapses according to ultrastructural criteria. Dendritic shafts were identified by their size and the presence of mitochondria and microtubules. Dendritic spines were of smaller diameter, lacked mitochondria and microtubules, and occasionally contained a spine apparatus. The axodendritic synapses comprised an insignificantly small proportion in all samples and therefore were excluded from further statistical estimation. All axospinous synapses were counted in each micrograph with exception of those touching the exclusion lines (an unbiased counting frame, Gundersen, H.J.G., *J. Microsc.* 111: 219-223, 1977). The cross-section areas of axonal terminals and postsynaptic spines and lengths of synaptic junctions of all axospinous synapses were measured directly from the prints using a magnetic tablet (Kurta) and the Macstereology 2.8 (Ranfurly Microsystems, UK) analysis program. The numerical density of synapses were

obtained using size-frequency method and formula $N_V = N_A/d$ (were N_A is a number of synaptic profiles per unit area and *d* is the average length of synaptic junctions; Colonnier, M. and Beaulieu, C., *J. Comp. Neurol.* 231: 175-179, 1985; DeFelipe, J., *et al., Cereb. Cortex* 9:722-732, 1999).

The number of synapses per cubic mm (mm^3) was significantly reduced in neurotrypsin-overexpressing mice (Fig. 17). In contrast, the numbers of synapses in control mice, *i.e.,* the parental lines used for the generation of the double transgenic (DTG) neurotrypsin-overexpressing mice (491-inact.Nt, 494-inact-Nt, and CMV-Cre) were the same as in wild-type mice. Therefore, these results indicate a significant reduction of synapses in the neurotrypsin-overexpressing mice.

Axonal terminal area was significantly reduced in neurotrypsin-overexpressing mice (Fig. 18). In contrast, the values in control mice, *i.e.,* the parental lines used for the generation of the double transgenic (DTG) neurotrypsin-overexpressing mice (491-inact.Nt, 494-inact-Nt, and CMV-Cre) were the same as in wild-type mice. Therefore, these results indicate a significant reduction of the presynaptic terminal size in the neurotrypsin-overexpressing mice.

Synaptic length was significantly reduced in neurotrypsin-overexpressing mice (Fig. 19). In contrast, the values in control mice (*i.e.,* the parental lines used for the generation of the double transgenic (DTG) neurotrypsin-overexpressing mice (491-inact.Nt, 494-inact-Nt, and CMV-Cre)) were the same as in wild-type mice. Therefore, these results indicate a significant reduction of the synaptic area in the neurotrypsin-overexpressing mice.

The cross sectional area of the postsynaptic spines was significantly reduced in neurotrypsin-overexpressing mice (Fig. 20). In contrast, the values in control mice, i.e. the parental lines used for the generation of the double transgenic (DTG) neurotrypsin-overexpressing mice (491-inact.Nt, 494-inact-Nt, and CMV-Cre) were the same as in wild-type mice. Therefore, these results indicate a significant size reduction of the postsynaptic spines in the neurotrypsin-overexpressing mice.

In summary, the synapse density, as determined by the number of synapses per mm^3, is significantly reduced in the neurotrypsin-overexpressing mice as compared with wildtype and control littermates (Fig. 17). The presynaptic terminals are reduced in size (Fig. 18). The synaptic length, as determined by the length of the apposition of the pre- and postsynaptic membrane, is significantly reduced in neurotrypsin-overexpressing mice (Fig. 19). Similarly, the size of the postsynaptic spines is significantly reduced in neurotrypsin-overexpressing mice (Fig. 20).

In transgenic mice overexpressing the catalytically inactive mutation of neurotrypsin, engineered by mutating the reactive site serine 711 to an alanine (Ser711Ala mutation), these synaptic alterations were not found. In conclusion, the observations made in transgenic

mice overexpressing the wild-type form of neurotrypsin are mediated by the proteolytic activity of neurotrypsin.

APPENDIX L

EXPERIMENT 11: Neurotrypsin cleaves agrin and reduces synaptic agrin (results revealed by Western blots).

In search for the proteolytic target proteins of neurotrypsin, we focused on extracellular proteins of the synaptic cleft or membrane proteins of the pre- and post-synaptic membranes. Because of the numerous parallels between CNS synapses and the neuromuscular junction, proteins thought to occur at both were included in the group of candidates, even if their characterization has been worked out exclusively or predominantly at the neuromuscular junction. Among the many candidates two are of primary relevance: Agrin and MuSK.

Agrin is a well-characterized synaptic organizer molecule of the neuromuscular junction (Sanes, J.R. and Lichtman, J., *Nat. Rev. Neurosci.* 2: 791 – 805, 2001). It has a core protein mass of 210 kDa. Recently, the expression of agrin in the brain and its role in synaptic development, structure and function has received considerable attention (Smith, M.A. and Hilgenberg, L.G., *Neuroreport* 13: 1485 – 1495, 2002; Kroger, S. and Schroder, J.E., *News Physiol. Sci.* 17: 207 – 212, 2002). Agrin exists in several isoforms. Most of these isoforms are extracellular matrix proteins, but there are also type II transmembrane forms that carry a very short N-terminal cytoplasmic segment. MuSK is a muscle-specific tyrosine kinase which functions as a putative receptor of agrin. The functional importance of agrin and MuSK is documented by the finding that knockout mice for either of these genes died around birth. Embryonic analysis of neuromuscular development revealed severe defects in the formation of neuromuscular junctions (Gautam, M. *et al.*, *Cell* 85: 525-535, 1996; DeChiara, T. M. *et al.*, *Cell* 85: 501-512, 1996). Recent studies in our laboratory led to the observation that neuromuscular junctions fail to form properly in neurotrypsin-overexpressing mice. Consequently, we hypothesized that a putative substrate of neurotrypsin should be detectable among the molecules present in the synaptic cleft or the surface membranes of the neuromuscular junction.

To test whether agrin is a substrate of neurotrypsin we developed a cotransfection assay with HEK293T cells. For this purpose, a 2310 bp KpnI-HindIII fragment just encompassing mouse neurotrypsin coding sequences was cloned into the eucaryotic expression vector pcDNA3.1(-) (Invitrogen) via KpnI and HindIII. A cDNA clone coding for rat agrin (the transmembrane isoform Y4, Z8) was obtained from Dr. K. Tsim (University of Hong Kong). In this clone, rat agrin is inserted into the polylinker of pcDNA3 (Invitrogen) via KpnI and EcoRI.

HEK293T cells were cultured in DMEM/10% FCS at 37°C in humidified air with 10% CO_2. For transfection, cells were seeded in 3 ml DMEM/10% FCS onto glass cover slips placed into a 3 cm dish. The day after seeding, at a confluence of 40-60%, the cells were transiently transfected with cDNAs encoding neurotrypsin and agrin (5 g DNA each) using

calcium-phosphate precipitation. Four hours after transfections, the medium was carefully removed and replaced by 3 ml fresh DMEM/10% FCS. Cells were further incubated for 48 hrs.

Immunofluorescence was used to investigate the impact of neurotrypsin on agrin distribution. Forty-eight hrs after transfection, the cells were fixed with 4% paraformaldehyde in PBS for 10 min. Excess of the fixative was removed by washing and quenching in PBS/glycine. After blocking with horse serum the cells were incubated with the primary antibodies (SZ177, rabbit anti-neurotrypsin antibody, 1:300; AGR540 (Stressgen), a mouse anti-agrin antibody, 1:600) for 45 min, washed with PBS, incubated with secondary Texas red-coupled anti-rabbit IgG and FITC-coupled anti-mouse IgG, respectively for 45 min, washed, and mounted onto glass slides with fluorescent mounting medium (DAKO).

Single cDNA transfection resulted in neurotrypsin immunoreactivity diffusely arranged around the cell (Fig. 22 A). Agrin immunofluorescence was found highly concentrated at the cell surface, as expected for an integral membrane protein (Fig. 22 B). Analysis after double transfection showed a rather different situation: cell surface agrin immunoreactivity was absent in neurotrypsin-positive cells (Fig. 22, C and D). Intracellular agrin immunoreactivity, however, was still detectable in neurotrypsin-positive cells (Fig. 22, E and F).

We repeated the assay using the cDNA coding for catalytically inactive neurotrypsin (a mutant in which the active-site serine is replaced by alanine). Single transfection showed that catalytically inactive neurotrypsin was produced and subcellularly distributed in a manner indistinguishable from wild-type neurotrypsin (not shown). In contrast to active neurotrypsin, however, double transfection with agrin and inactive neurotrypsin did not result in the disappearance of agrin from the cell surface (Fig. 22, G-K).

Immunodetection of agrin in transfected HEK293T cells was done with two different anti-agrin antibodies with virtually identical results. Both antibodies recognize an epitope located in the extracellular C-terminal third of the protein. Thus, neurotrypsin-mediated cleavage must occur N-terminally to these epitopes to release a C-terminal portion of agrin. Additionally, in neurotrypsin transfectants, immunoreactivity was only loosely associated with the cell periphery (Fig. 22A). In the presence of agrin, however, neurotrypsin (both active and inactive form) was clearly enriched at the plasma membrane (Fig. 22, C,E,G,I).

From this finding, we conclude that the disappearance of cell surface agrin is caused by neurotrypsin-mediated proteolysis within the extracellular domain of agrin. The redistribution of neurotrypsin in the presence of overexpressed agrin furthermore suggests that agrin influences neurotrypsin targeting, possibly by acting as a direct or indirect binding partner at the cell surface or by acting as a carrier for neurotrypsin secretion.

We then performed Western blot analysis to follow the fate of agrin biochemically. For this purpose, HEK293T cells were directly seeded into 3 cm wells and cultured in 2 ml

DMEM/10% FCS. Transfection was performed as described for immunofluorescence analysis. 48 hrs after transfection, the cells were washed with PBS. The cells were lysed by the addition of 250 l buffer (20 mM Tris-HCl, pH 7.4, 150 mM NaCl, 1 mM EDTA, 1% Triton X-100, protease inhibitor cocktail). The extract was incubated at 4°C for 20 min and then centrifuged for 20 min with 15000 x g at 4°. The supernatant was saved. After determination of protein concentration, the supernatant was mixed with 5 x Laemmli loading buffer, boiled for 3 min, centrifuged and used for analysis. Proteins were separated by SDS-PAGE, using 7.5% acrylamide. After electrophoresis, proteins were transferred to a nitrocellulose membrane. Transfer quality was verified by Ponceau S staining. The membrane was then blocked with TBS containing 0.1% Tween-20 and 5% (w/v) blocking reagent (Amersham). All subsequent steps were done in TBS with 0.1% Tween-20. The membrane was incubated with the primary antibody (SZ177, 1:1000; AGR540, 1:1000; K-17, a polyclonal anti-agrin antibody (Santa Cruz), 1:1000) for 60 min. After extensive washing, the membrane was incubated with secondary peroxidase-coupled antibodies for 45 min. Detection was done with ChemiGlow (Alpha Innotech) according to the manufacturer's instruction. Images were taken with a ChemiImager (Alpha Innotech).

Agrin was clearly identified in detergent extracts of single transfectants (Fig. 23, lane 1). In extracts of double transfectants, agrin was strongly reduced (Fig. 23, lane 2). No agrin signal was found in cells transfected with empty vector (Fig. 23, lane 3). The production of neurotrypsin under all conditions was confirmed after reprobing the blot with anti-neurotrypsin antibodies (not shown). In 200 l culture medium of double transfected HEK293T cells a 100 kDa signal was detected with the anti-agrin antibody (Fig. 23, lane 5). This signal was not found in medium from single transfectants (Fig. 23, lane 4). Likewise, no signal was detected in medium of HEK293T cells transfected with agrin and catalytically inactive neurotrypsin (Fig. 23, lane 6). Lanes 7 and 8 are as lane 5 with only 100 l and 50 l medium, respectively.

In summary, the results from the immunofluorescence and Western blot analysis indicate that:

1) neurotrypsin produced in HEK293T cells has catalytic activity;

2) agrin, an extracellularly-present component of the neuromuscular junction and the synapses of the central nervous system, can be cleaved by neurotrypsin-dependent proteolysis; and

3) this neurotrypsin-dependent cleavage leads to the formation of a truncated and a released form of agrin.

Because the released portion of agrin contains the domain bearing the synaptogenic site of agrin, these results indicate that the synaptic changes induced by the overexpression of

neurotrypsin in neurons are due to the neurotrypsin-dependent proteolysis and indicate a regulatory role of neurotrypsin for synaptic structure and function.

APPENDIX M

EXPERIMENT 12: Production of neurotrypsin

Neurotrypsin is a secreted multi-domain protein with a length of 875 amino acids and an estimated size of 97 kDa for human neurotrypsin and 761 amino acids and a size of 85 kDa for mouse neurotrypsin (Fig. 24). The expression of this serine protease as an active protein is dependent upon proper folding and very likely on post-translational modifications, e.g. N-glycosylation which has been proposed for 2 sites in the case of the human and 3 sites for the mouse protein (Gschwend, T.P. *et al.*, *Mol. Cell. Neurosci.* 9, 207-219, 1997; Proba K., *et al.*, *Biochim. Biophys. Acta* 1396, 143-147, 1998). In addition, neurotrypsin contains a signal peptide directing the protein to the endoplasmatic reticulum from where it is secreted. Neurotrypsin is not an integral membrane protein since it is lacking a transmembrane domain as determined by a hydrophobicity plot by Kyte and Doolittle (Kyte, J. and Doolittle, R.F., *J. Mol. Biol.* 157, 105-132, 1982). The zymogen activation site of neurotrypsin shows high similarity to the one of tPA (tissue-type plasminogen activator; Tate, K.M. *et al.*, *Biochemistry* 26, 338-343, 1987). Cleavage at this site by a protease leads to the two fragments, one containing the non-catalytic domains with an apparent molecular weight of 55 kDa (for mouse neurotrypsin) or 67 kDa (for human neurotrypsin) and one containing only the protease domain with 30 kDa (Fig. 24). This two-chain form is still linked by a disulfide bond (Fig. 27.B).

The biochemical analysis of human neurotrypsin requires protein amounts in the milligram to gram range. Because proper folding and secretion of proteins depends on many, not yet fully understood cellular and molecular mechanisms, several eukaryotic expression systems have been tested for optimal production and secretion of neurotrypsin, including baculovirus-mediated expression in insect cells, stable expression in mouse myeloma cells, and transient expression in human embryonic kidney cells (HEK). These systems have the advantage that they can easily be adapted to serum-free conditions to reduce the amount of contaminating proteins in the supernatant and to set-ups for large-scale production.

1. Production of neurotrypsin in the human embryonic kidney cell lines HEK293T and HEK293-EBNA

An expression system for transient expression of recombinant protein in the human embryonic kidney cell lines HEK 293T or HEK 293-EBNA has been established. This system has been used with great success not only for the expression of cytosolic proteins, but also for transmembrane and secreted proteins (Batard, P. *et al.*, *Gene* 270, 61-68, 2001; Meissner, P., *et al., Biotechnol. Bioeng.* 75, 197-203, 2001). The gene of interest is delivered to the cells by calcium phosphate (CaPi) transfection with efficiencies between 70 - 100%. The plasmid encoding for the recombinant protein that is to be expressed stays episomally and is expressed from either a cytomegalovirus (CMV) or EF-1 alpha promoter. These

human-based expression systems have the advantage that post-translational modifications are very likely to be identical to modifications made by their natural producer cells. In addition, these systems are not only suitable for small-scale expression, but also for large scale production in suspension cultures (e.g. spinnerflasks 100 to 1000 ml or bioreactor 1 to 5 liter scale).

In pilot experiments, HEK 293T cells were transfected with a pcDNA3.1 (Invitrogen) vector encoding for neurotrypsin fused to a C-terminal histidine tag by CaPi. Cells were harvested 72 hrs post transfection. Western analysis using the anti-Tetra-His antibody (QIAGEN) detected an 85 kDa signal corresponding to the full-length mouse neurotrypsin in the cell extract and media supernatant (Fig. 25).

Expression of neurotrypsin has also been exploited by transient transfection of HEK293-EBNA cells. It has been reported that under optimized conditions of the transfection protocol and growth of HEK cells in suspension culture yields of >20 mg/l for secreted proteins, e.g. an IgG1-type human antibody, can be achieved (Meissner, P., *et al., Biotechnol. Bioeng.* 75, 197-203, 2001). This technology represents a rapid alternative to the widely used stable expression based on chromosomal integration of foreign DNA, which is costly and time consuming. The coding region of for the high level expression of mouse neurotrypsin fused to a C-terminal histidine tag was cloned into the pEAK8 vector (Edge Biosystems) under control of the EF-1 alpha promoter, which then is used to transfect HEK293-EBNA cells. Cells and supernatants were harvested 5 days post-transfection. Under reducing conditions full-length neurotrypsin is detected at 85 kDa in the cell extract, while in the supernatant a 55 kDa band is detected using a neurotrypsin-specific antibody directed against the basic proline-rich domain (Fig. 26). This fragment of neurotrypsin corresponds to the expected size of the non-catalytic fragment after cleavage.

2. Production of neurotrypsin in insect cells by infection with recombinant baculovirus

Recombinant baculoviruses are widely used for the expression of heterologous genes cultured in insect cells. Advantage of this system is not only the similarity of post-translational modifications to those of mammalian cells which can be optimized on a case to case basis (Ailor, E. and Betenbaugh, M.J., *Curr. Opin. Biotechnol.* 10, 142-145, 1999), but also that insect cells can easily be adapted to suspension culture in roller bottles, shaker flasks, or to bioreactor settings for high-level expression. Expression of the gene of interest is driven by the powerful polyhedrin promoter, which is transcriptionally active in the late phase of virus propagation. It has already been demonstrated for the serine protease neuropsin that high level expression of secreted and biologically active protein can be obtained from baculovirus infected insect cells (Shimizu, C., *et al., J. Biol. Chem.* 273, 11189-11196, 1998). Yields of 4 mg/l in adherent baculovirus-based system could be obtained from adherent cultures

expressing secreted Lep d2 protein (Olsson, S. *et al.* (1998), *Clin. Exp. Allergy* 28, 984-991, 1998). The percentage of active secreted protein was determined in the range of 50-90% for recombinant secreted gp120 (Golden, A. *et al.*, *Protein Expr. Purif.* 14, 8-12, 1998).

The coding region for neurotrypsin was inserted into the pFASTbac1 vector (Invitrogen). After recombination of the neurotrypsin-coding region into the baculovirus genome insect cells were transfected and recombinant virus harvested. High5 insect cells (Invitrogen) are infected at a MOI (Multiplicity of infection) of 4. Three days post-infection cells and supernatant are collected. Full-length neurotrypsin is detected (Fig. 27). When probing with an antibody binding to the proline-rich basic domain, full-length neurotrypsin and the non-catalytic fragment at 55 kDa is detected (Fig. 27A and 27B). Using an antibody specific for the protease domain a band at 30 kDa is observed, corresponding to the calculated molecular weight of the protease domain. Under non-reducing conditions, only one band for neurotrypsin is detected (Fig. 27B) indicating that the cleaved fragments are still linked by the disulfide bridge formed by residues Cys505 and Cys520 (Fig. 24).

3. Production of neurotrypsin in myeloma cells

A stable expression system that is being exploited is a myeloma-based system, which had already been successfully used within our group to express secreted, recombinant axonin-1 variants (Rader C. *et al.*, *EMBO* 15: 2056-2068, 1996; Freigang J. *et al.*, *Cell* 101: 425-433, 2000). This system had been developed based on the rational that mouse myeloma cells are the professional secretory cells in an organism (Traunecker, A., *et al.*, *Biotechnol.* 9, 109-113, 1991). Thus, there have been reports that some mouse myeloma cell lines can produce 100mg/l of secreted protein. The best-suited cell line is mouse myeloma J558L line which can be transfected by protoplast fusion (Oi, V.T. *et al.*, *Proc. Natl. Acad. Sci.* USA 80, 825-829, 1983).

For the stable transfection of myeloma cells the coding region of mouse and human neurotrypsin was inserted into a specially designed vector (Traunecker, A., *et al.*, *Biotechnol.* 9, 109-113, 1991). Expression by this vector is driven by an Ig κ light chain promoter and enhancer. The 3' end of the transcript of interest is spliced onto an exon encoding the Ig κ constant domain in order to mimic stable Ig transcripts. The vector contains a histidinol dehydrogenase gene that allows the selection of stable transfectants in the presence of L-histidinol. L-histidinol is a precursor of L-histamine and an inhibitor of protein synthesis. The vector has been stably transfected by protoplast fusion into the mouse myeloma cell line J558L (ECACC #88032902; European Collection of Cell Cultures, Salisbury, UK) for the production of recombinant neurotrypsin. Transfection by protoplast fusion is a highly efficient method for the direct transfer of mammalian expression vectors from bacteria to mammalian cells (Schaffner (1980), *Proc. Natl. Acad. Sci.* USA 77, 2163-2167; Sandri-Goldin *et al.*

(1981), *Mol. Cell. Biol.* 1, 743-752; Rassoulzadegan *et al.* (1982), *Nature* 295, 257-259; Gillies *et al.* (1983), *Cell* 33, 717-728). It involves digesting bacterial cell walls with lysozyme to produce protoplasts and then fusing the protoplasts to mammalian cells in the presence of polyethylene glycol. Here we used the mouse myeloma cell line J558L. Other suitable lines for stable transfection by protoplast fusion or electroporation include mouse P3-X63Ag8.653, mouse Sp2/0-Ag14, mouse NSO, and rat YB2/0 (Gillies *et al.* (1989), *Biotechnology* 7, 799-804; Nakatani *et al.* (1989), *Biotechnology* 7: 805-810; Bebbington *et al.* (1992), *Biotechnology* 10: 169-175; Shitara *et al.* (1994), *J. Immunol. Meth.* 167, 271-278).

The following protocol is based on the myeloma expression system described by Traunecker *et al.* (1991), *Biotechnol.* 9, 109-113 and can easily be adapted to other systems. For the preparation of protoplasts the glycerol stock of an *E. coli* strain 803 clone containing the mammalian expression vector is streaked on a LB agar/ampicillin plate and grown overnight at 37°C (strain 803 available from ATCC #35581). One single colony is inoculated in 2 ml pre-warmed (37°C) LB media containing 50 g/ml ampicillin. After 4 hrs shaking at 250 rpm and 37°C 100 µl of the culture is transferred to 100 ml fresh media. After the culture reached an optical density (OD at 600 nm) of about 0.6, chloramphenicol is added to a final concentration of 120 µg/ml and grown overnight at 250 rpm and 37°C. Plasmids carrying the colE1 origin of replication can be amplified in the presence of chloramphenicol (Hershfield *et al.* (1974), *Proc. Natl. Acad. Sci. USA* 71, 4355-3459).

The overnight culture is centrifuged at 2500 g for 10 min at 4°C. The pellet is resuspended in 2.5 ml ice-cold 20% (w/v) sucrose in 50 mM Tris-HCl, pH 8.0. Five hundred µl ice-cold 1 mg/ml lysozyme in 250 mM Tris-HCl, pH 8.0, are added followed by an incubation on ice for 5 minutes. After addition of 1 ml ice-cold 250 mM EDTA, pH 8.0, and incubation on ice for 5 minutes, 1 ml ice-cold 50 mM Tris-HCl, pH 8.0, is added and the protoplast preparation incubated at room temperature for 10 minutes. During this incubation period, formation of spherical protoplasts from the usually rod-shaped bacteria can be observed using a microscope with 1000 x magnification. About 90% protoplasts should be formed at the end of the incubation period. To the protoplast suspension 20 ml DMEM supplemented with 10% (w/v) sucrose, 10 mM $MgCl_2$ and 40 l 10mg/ml DNasel is added. After incubation for 15 min at room temperature, the protoplast preparation is spun at 2500 g for 30 min at room temperature.

In the meantime, myeloma cells J558L are prepared for the fusion. Myeloma cells were grown in DMEM supplemented with 10% (v/v) FCS and should reach a high cell density of approximately 1 x 10^6 cells/ml on the day of transfection. Per protoplast fusion 5 x 10^6 cells are spun down at 500 g for 10 minutes at room temperature. The cells are resuspended in 5 ml pre-warmed DMEM (37°C) and slowly layered on top of the protoplast pellet after the last centrifugation. To mix protoplasts and myeloma cells they are spun at 500 g for 10 min at

room temperature. After removal of the supernatant the cells are mixed by flicking the tube. For the fusion 2 ml PEG 1500 in DMEM supplemented with 10% DMSO is added and the pellet resuspended by pipetting up and down several times. About 1 to 2 min after addition of the PEG solution, 10 ml pre-warmed DMEM (37°C) media is added slowly. After 10 ml pre-warmed DMEM supplemented with 10% (v/v) FCS (37°C) is added the fusion is centrifuged at 500 g for 10 min at room temperature. The supernatant is removed by aspiration and the pellet resuspended in 50 ml pre-warmed DMEM supplemented with 10% (v/v) FCS (37°C) and 100 µl 50 mg/ml kanamycin. Finally, the cells are distributed among five 96-well tissue culture plates by adding 100 µl/well using a multipipette. After 48 hrs incubation in a humidified incubator at 37°C with 10% CO_2, L-histidinol is added in a final concentration of 5 mM. Only transfected myeloma cells will survive the treatment with L-histidinol. Clones are visible about 12 to 14 days after the selection had started.

On average 40 to 50 clones are obtained per protoplast fusion. All clones were analyzed for expression by Western with neurotrypsin-specific antibodies. While the majority of myeloma cell clones expressed no or only moderate amounts of neurotrypsin, a small percentage of 5-10% revealed a very high expression level. Clones with high expression level were subcloned over three rounds of single cell dilutions to ensure the stability of neurotrypsin expression.

From the stably expressing clones cells and supernatant was collected. Both were separated on a 10% SDS PAGE and probed with neurotrypsin specific antibodies (Fig. 28). While full-length neurotrypsin is predominately detected in the cell extract, the 55-kDa band of the non-catalytic fragment is detected in the media supernatant when probing with an antibody against the N-terminal proline-rich basic domain. A band at 30 kDa is detected with an antibody directed against the protease domain, corresponding to the calculated molecular weight of the protease domain. Similar results are obtained with human neurotrypsin.

4. Additional ways to produce recombinant neurotrypsin

Alternatively, expression in eucaryotic cells may be achieved with a variety of eucaryotic expression vectors (commercially available or self-made). Likewise, a variety of eucaryotic cell lines may be used, including COS cells, CHO cells, HeLa cells, H9 cells, Jurkat cells, NIH3T3 cells, C127cells, CV1 cells, or Sf cells. For a detailed description of the use of COS cells or CHO cells, or a baculovirus-based expression system see International Application Number PCT/US96/16484 or International Publication Number WO 98/16643. In addition, the expression of neurotrypsin is also possible in yeast expression systems. The EasySelect™ Pichia Expression kit (Invitrogen, cat. No. K1740-01) is used for this purpose. However, expression systems of other suppliers may be used alternatively. The coding region of human neurotrypsin, excluding the natural signal sequence, was inserted into the

pPICZα vector in frame with the -factor signal sequence. High-level expression of the gene of interest is driven by the AOX1 promoter. The AOX1 promoter drives expression of alcohol oxidase in Pichia, an enzyme that catalyzes the first step in methanol metabolism. The gene of interest can be inducibly expressed by addition of up to 2% of methanol to the culture media.

5. Production of neurotrypsin from a human cell line with endogenous expression of neurotrypsin

The production of neurotrypsin may also be based on mammalian cell lines exhibiting endogenous expression of neurotrypsin. Expression of endogenous human neurotrypsin has been observed at the RNA level in the human mast cell line HMC-1 (Butterfield, J.H. *et al.*, *Leuk. Res.* 12, 345-355, 1988; Poorafshar, M. and Hellman, L., *Eur. J. Biochem.* 261, 244-250, 1999). The HMC-1 cell line represents a naturally occurring source for properly processed and, therefore, very likely for active human neurotrypsin. These cells can be grown in suspension culture and constitutively express human neurotrypsin. The protein expressed from HMC-1 cells can be detected as 97-kDa band by a specific polyclonal antibody raised against the kringle domain in Western experiments (Sales, unpublished data). After fractionation of supernatant, cell lysate and membranes neurotrypsin localized with the membrane fraction. When the membranes are stripped under acidic conditions (200 mM glycine, pH 2.2, 1% Tween 20, 0.1% SDS) neurotrypsin can be detected in the soluble rather than the insoluble fraction, indicating a secreted and membrane-associated protein. Neurotrypsin can be purified to homogeneity from the supernatants of stripped membranes by several chromatographic steps.

However, since HMC-1 cells represent a natural source for human neurotrypsin expression coupled with the correct post-translational processing machinery, these cells are used to stably express recombinant neurotrypsin at a higher level than the endogenous gene. To this purpose HMC-1 cells are transfected with the vector pcDNA3.1 (Invitrogen) encoding for human neurotrypsin containing the neomycin resistance gene for selection with G418. It has been shown that HMC-1 cells can be transfected by electroporation (Ali, H. *et al.*, *J. Immunol.* 165, 7215-7523, 2000). In addition, other proteins have been successfully expressed in HMC-1 cells, e.g. recombinant human proteinase 3. This protein was conformationally intact and active (Specks, U. *et al.*, *FEBS* 390, 265-270, 1996).

APPENDIX N

EXPERIMENT 13: Purification of neurotrypsin

All the expression systems that we tested in our pilot experiments, HEK293-EBNA, baculovirus-mediated expression in insect and myeloma cells, can be scaled up for large scale production of recombinant neurotrypsin. Neurotrypsin is then purified from the supernatant. Thus, the adaptation of the cells producing recombinant neurotrypsin to growth in serum-free medium, if possible, represents a major advantage for the production and purification of neurotrypsin.

For example, 1 liter supernatant derived from the myeloma expression system contains 500 mg total protein. As a first purification step, affinity purification on a heparin column is used. Other proteases, e.g. thrombin, have already been purified successfully using a heparin column (Ding, Z., *et al.*, *Prep. Biochem.* 25: 21-28, 1995). As a second chromatographic step, an arginine sepharose 4B column was used. The eluted protein was then further purified by ion exchange chromatography on a Mono S column followed by hydrophobic interaction chromatography. Depending on the experimental requirements, additional or alternative chromatography steps on ion exchange (DEAE or Mono Q) columns or by gel filtration have also been found useful for the purification of neurotrypsin.

The source of neurotrypsin used was a conditioned cell culture supernatant resulting from the cultivation of a neurotrypsin-expressing myeloma cell line. These cells have been adapted to growth in a serum-free medium (Stoll, T.S. *et al.*, *J. Biotechnol.* 45: 111-123, 1996; Ackermann, G.E. and Fent, K., *Marine Environmental Research* 46: 363-367, 1998) in the TechnoMouse fermenter (Integra Biosciences), originally developed for the large-scale production of monoclonal antibodies. Starting from a medium composed of DMEM (Gibco, nr. 41966-029) containing 2 mM glutamine and 10 % FCS, the cells were stepwise adapted to grow in this medium with 1 % FCS. Adaptation was performed in 24 well plates and the medium was exchanged approximately every second day. When cells reached confluency, they were split into another well. Throughout the whole procedure, cells were kept at a density near confluency.

Adapted cells growing well in DMEM containing 1 % FCS were then transferred to the serum-free, but protein- containing, medium HL-1 (Bio-Whittacker, nr. 77201) supplemented with 0.5 % FCS. In HL-1 medium the cells were then stepwise adapted to grow in HL-1 medium only (without FCS). To adapt the cells to the protein-free medium TurboDoma (Cell Culture Technologies GmbH, Zurich, nr. THP) the HL-1 medium was stepwise exchanged by TurboDoma. The adaptation steps from HL-1 to TurboDoma medium were performed analogously to the reduction of FCS.

In detail, the following conditions were used for the chromatographic purification of recombinant neurotrypsin:

1. Affinity chromatography on heparin sepharose

As the first purification step a heparin sepharose CL-6B column was used (Amersham Pharmacia Biotech, nr. 17-0467-01). The bed volume was 80 ml and the column was run on the FPLC chromatography system. Immediately following collection from the fermenter, the pH of the conditioned medium was adjusted to 6.5 by using 1 M MES, pH 6.5, resulting in a final concentration of 50 mM. The loading buffer was 50 mM sodium chloride in 20 mM MES, pH 6.5, whereas the elution buffer contained 1 M NaCl in 20 mM MES, pH 6.5. We used a linear gradient starting at a concentration of 50 mM sodium chloride and ending at 1 M sodium chloride over a total volume of 320 ml. The eluted fractions were screened for the presence of neurotrypsin by Western blotting using an antibody against the proline-rich basic domain. For confirmation, Western blots were repeated with selected fractions using antibodies against the kringle domain and antibodies against the protease domain. The fractions containing neurotrypsin were prepared for the next step, the arginine affinity chromatography, by dialysis versus an excess of 50 mM sodium chloride in 20 mM MES, pH 6.5.

2. Affinity chromatography on arginine sepharose

The arginine affinity chromatography was carried out using an arginine sepharose 4B column (Amersham Pharmacia Biotech, nr. 17-0524-01) with a bed volume of 18 ml. The loading buffer was 50 mM sodium chloride in 20 mM MES at pH 6.5. For elution, a gradient was used with 4 column volumes from 0 to 150 mM arginine and with 3 column volumes from 150 to 200 mM arginine. The column was regenerated with 1 M sodium chloride. The eluted fractions were screened for the presence of neurotrypsin by Western blotting using an antibody against the proline-rich basic domain. For conformation, Western blots were repeated with selected fractions using antibodies against the kringle domain and antibodies against the protease domain. The fractions containing neurotrypsin were prepared for the next step, the MonoS ion exchange chromatography by dialysis versus an excess of 50 mM sodium chloride in 20 mM MES, pH 6.5.

3. Ion exchange chromatography on the strong cation exchanger MonoS

The strong cation exchanger MonoS was used with a column volume of 1 ml (MonoS HR 5/5, Amersham Pharmacia Biotech, nr. 17-0547-01). The loading buffer contained 50 mM sodium chloride in 20 mM MES, pH 6.5. The elution buffer contained 1 M sodium chloride in 20 mM MES, pH 6.5. Elution was by a linear gradient starting at 50 mM sodium chloride and ending at 1 M sodium chloride after 40 column volumes. The eluted fractions were screened for the presence of neurotrypsin by Western blotting using an antibody against the proline-rich basic domain. For confirmation, Western blots were repeated with selected fractions

using antibodies against the kringle domain and antibodies against the protease domain. The fractions containing neurotrypsin were prepared for the next step, the hydrophobic interaction chromatography by dialysis versus an excess of 50 mM sodium chloride, 1 M ammonium sulfate in 20 mM MES, pH 6.5.

4. Hydrophobic interaction chromatography on the hydrophobic interaction matrix butyl sepharose

A HiTrap butyl sepharose column with a bed volume of 1 ml was used (Amersham Pharmacia Biotech, nr. 17-1357-01). The loading buffer consisted of 50 mM sodium chloride and 1 M ammonium sulfate in 20 mM MES, pH 6.5. The elution buffer was 50 mM sodium chloride, 20 mM ethylene glycol in 20 mM MES, pH 6.5. A linear gradient over 20 column volumes from 1 M to 0 M ammonium sulfate was used. The eluted fractions were screened for the presence of neurotrypsin by Western blotting using an antibody against the praline-rich basic domain. For confirmation, Western blots were repeated with selected fractions using antibodies against the kringle domain and antibodies against the protease domain. This procedure was used to purify recombinant neurotrypsin produced by the stably transfected myeloma cell line J558L. Neurotrypsin produced by a number of other recombinant expression systems (mentioned above), as well as neurotrypsin from cell lines naturally expressing neurotrypsin, e.g. the mast cell line MHC-1, and neurotrypsin from the murine, rat and bovine brain may be successfully purified using the same or a modified procedure. Neurotrypsin from animal tissue may require additional chromatographic steps, such as ion exchange chromatography on a DEAE-substituted matrix, such as DEAE-sepharose or Bio-Gel SEC DEAE-5-PW (Biorad), or on a MonoQ anion exchange column (Amersham-Pharmacia), or by gel filtration.

APPENDIX O
FIGURES

Fig. 1
The mRNA encoding neurotrypsin is shown in a coronal section of the brain of an adult mouse by *in situ* hybridization using DIG-labeled neurotrypsin antisense cRNA. The coronal section shows the superior colliculus (SC), the thalamus, and the hypothalamus. Labeling is seen in distinct layers throughout the neocortex (Te, temporal cortex; Oc, occipital cortex) with a more widespread labeling in the transition zones between iso- and allocortex (Ic, insular cortex; RS, retrosplenial cortex). In the allocortex, labeling is detected in the piriform cortex (Pir), with a strong labelling in the endopiriform nucleus (arrow), and in the hippocampal formation (S, subiculum; Hc, hippocampus). Strong neurotrypsin expression is also seen in the lateral amygdala (LA).

Fig. 2
The localization of neurotrypsin protein in the brain of an adult mouse is shown in a coronal section by immunolabeling with a specific, affinity-purified antibody against neurotrypsin and a peroxidase-conjugated secondary antibody. A strong immunoreactivity is visible in the gray matter. Particularly strong neurotrypsin immunoreactivity can be seen in the cerebral cortex (C), and the hippocampus (Hc). However, many other regions of the brain exhibit neurotrypsin immunoreactivity. Moderate neurotrypsin immunoreactivity is found in the lateral geniculate nucleus (LGN). High neurotrypsin immunoreactivity is found in the medial (MEA) and basomedial (BMA) nuclei of the amygdala, in the caudate putamen (CP), and in the substantia nigra (SN). No staining for neurotrypsin was detected in the white matter.

Fig 3
The localization of neurotrypsin protein is demonstrated in the hippocampus of an adult mouse. (A) Neurotrypsin was visualized in a coronal section of the hippocampus by immunolabeling with a specific, affinity-purified antibody against neurotrypsin and a peroxidase-conjugated secondary antibody. A strong immunoreactivity was found in the synaptic layers. (B) A higher magnification view at the stratum radiatum (s.r. in panel A) of the hippocampus is shown. The pyramidal cells of the CA1 region are marked (Pc), in order to allow the identification of the location of the investigated tissue. Neurotrypsin immunoreactivity can be seen distributed in small discrete spots. The strong punctuate immunolabeling of the neuropil is typical for a protein with a synaptic localization. The neuronal somata of the pyramidal cells (Pc) of the CA1 region were unlabeled.

Fig. 4
The localization of neurotrypsin is shown by immuno-electron microscopy of the stratum radiatum (s.r. in Fig. 3A) of the CA1 region of the hippocampus of an adult mouse. Neurotrypsin was visualized using preembedding staining with a specific, affinity-purified antibody against the proteolytic domain of neurotrypsin and a peroxidase-conjugated secondary antibody. The neurotrypsin immunoreactivity is found at presynaptic sites of axospinous and axodendritic asymmetric synapses. The immunoperoxidase reaction product is associated with the presynaptic membrane and the active zone of the presynaptic terminal (arrows). (Pre, presynaptic axon terminal; Post, postsynaptic spine).

Fig. 5
The localization of neurotrypsin is shown by immunogold-electron microscopy of the stratum radiatum (s.r. in Fig. 3A) of the CA1 region of the hippocampus of an adult mouse. The synaptic localization of neurotrypsin was confirmed. Neurotrypsin was visualised using specific, affinity-purified primary antibody against the protease domain and 1.4 nm gold-conjugated secondary antibody, followed by silver intensification. Neurotrypsin accumulates within the presynaptic active zones of the axonal terminals that form asymmetric (arrows) synapses with dendritic spines (sp, A and B) and dendritic shafts (dend, D and E), and symmetric (arrowheads) synapses with neuronal somata (C and F). Scale bar, 0.2 μm.

Fig. 6
The synaptic localization of neurotrypsin in the human brain is demonstrated by light- and electron-microscopic immununocytochemical visualization. Neurotrypsin was visualized in adult human cerebral cortex using preembedding immuno-EM staining with a specific, affinity-purified antibody against the proteolytic domain of neurotrypsin. (A) Immunohistochemical visualization of neurotrypsin with peroxidase-conjugated secondary antibody. The strong punctate immunolabeling of the neuropil is typical for a protein with synaptic localization. Neuronal somata (marked by asterisks) were unlabeled. (B) Preembedding immuno-EM localization by immunoperoxidase demonstrates the localization of neurotrypsin at presynaptic sites of axospinous and axodendritic asymmetric synapses in the cerebral cortex. The immunoperoxidase reaction product is associated with the presynaptic membrane and the active zone of the presynaptic terminal (arrows). (C) Immuno-gold localization of neurotrypsin at selected synapses. Note the exclusive labeling of presynaptic terminals in the region lining the synaptic cleft. Scale bars, 0.5 μm.

Fig. 7
The localization of neurotrypsin in synaptosomes and synaptic membranes is shown by differential centrifugation of brain homogenate. Starting with brain homogenate of wild-type mice, synaptosomes, synaptic membranes, and synaptic vesicles were isolated by differential centrifugation following established protocols. The presence of neurotrypsin in the subcellular fractions was determined by Western blotting, using a specific antibody against the proline-rich basic domain of neurotrypsin. In order to control for the correct tissue fractionation, synaptophysin, a component of the presynaptic vesicles, and NR1 (a subunit of the NMDA-type glutamate receptor), a component of the postsynaptic membrane, were tested on the same fractions. Note the enrichment of the synaptic membrane marker NR1 along the purification process, cumulating in the synaptic membrane (SPM) fraction, i.e. from the brain homogenate (H), via the homogenate supernatant free of nuclear pellet (S1), to the crude synaptosomes (P2'), to the crude synaptic plasma membranes (LP1), to the purified synaptic plasma membrane (SPM). Note also the enrichment of the synaptic vesicle marker synaptophysin along the purification process, cumulating in the synaptic vesicle (SV) fraction, i.e. from the brain homogenate (H), via the homogenate supernatant free of nuclear pellet (S1), to the crude synaptosomes (P2'), to the crude synaptic vesicles (LP2), to the purified synaptic vesicles (SV). The minor band of synaptophysin in the synaptic membrane fraction is in accordance with the expectations, because approximately 10 % of the synaptophysin is located in the presynaptic membrane, due to the constant fusion of synaptic vesicles into the presynaptic membrane. The double band observed in the initial fractions (S1, P2', LP1, and LP2) indicates a processing of neurotrypsin along its secretory pathway. In the plasma membrane fraction, almost all neurotrypsin was present in the lower molecular weight form, indicating that the lower molecular weight form represents the mature form of neurotrypsin. H, brain homogenate; S1, brain homogenate supernatant free of nuclear pellet; P2', crude synaptosomes; LP1, crude synaptic plasma membrane; LP2, crude synaptic vesicles; SV, synaptic vesicles, purified with sucrose gradient; SPM, synaptic plasma membrane purified with sucrose step gradient; Nt control, P2' fraction of neurotrypsin(Serine711Alanine)-overexpressing mouse.

Fig. 8
Transgenic constructs and the generation of neurotrypsin-overexpressing mice. On the upper left the figure the construct for the conditional overexpression of neurotrypsin is shown. Conditional overexpression indicates that the transgene is inserted into the mouse genome in an inactive form. In this conditional transgene, the coding part of the neurotrypsin cDNA was incorporated into the Thy1 gene and, thus, put under the control of the Thy1 promoter. In the graph, the first box marked by Thy1 indicates the transcription-regulating promoter at the 5' end of the Thy-1 gene. The second box marked by Thy1 indicates the 3' terminal sequences of the Thy1 gene. Between the Thy-1 promoter and the cDNA encoding neurotrypsin, a stop codon flanked by two loxP sequences was inserted. Transcription from the Thy-1 promoter of

this transgene, thus, stops before reaching the coding sequence of neurotrypsin. The inactive transgene can be converted into an active transgene by Cre recombinase. Cre recombinase promotes recombination at the loxP sites and, thus, excision of the transcriptional stop sequence. On the upper right side, the construct for expression of Cre-recombinase under the control of the cytomegalovirus (CMV) promoter is shown. Therefore, activation of the inactive transgene can be obtained by crossing the mice containing the inactive Thy1-neurotrypsin (inact.Nt) transgene with the mice containing the CMV-Cre transgene. If a heterozygous inact.Nt mouse is crossed with a heterozygous CMV-Cre mouse, the double-transgenic mice among the offspring express the Thy1-neurotrypsin transgene in the activated form. The expressed Cre-recombinase deletes the transcriptional stop sequence by promoting recombination at the loxP sequences. One loxP sequence remains within the activated Thy1-neurotrypsin transgene. The removed segment composed of the other loxP sequence and the transcriptional stop sequence is shown on the right. The mice were genotyped with the PCR method. The dashed arrows mark the region of the oligonucleotide primers used in the PCR.

Fig. 9
Schematic representation of a hippocampal slice and the electrode positions used in electrophysiological recordings. The electrophysiological investigations were performed on the Schaffer collateral pathway of the hippocampus. Positions of the stimulating (Stim) and recording electrodes and the cut introduced between the CA1 and the CA3. (DG, dentate gyrus; EC, entorhinal cortex; MF, mossy fibers; Mol, stratum moleculare; PP, perforant path; Sch, Schaffer collaterals; SP, stratum pyramidale; SR, stratum radiatum. The actual recordings took place at the border between the stratum radiatum and the stratum lacunosum-moleculare.

Fig. 10
fEPSP-peak time courses of a typical LTP induction in hippocampal slices of control and neurotrypsin-overexpressing mice. (A) Means of the raw fEPSP from a hippocampal control slice before and after induction of LTP: The first trace corresponds to 60 stimulations during baseline recording, the second to 240 stimulations after the induction of LTP. The dashed line in the second trace represents the baseline trace. (B) The fEPSP was evoked and recorded every 30 seconds, and the peak amplitudes represented by the middle third of the initial fEPSP slopes were displayed with respect to time. LTP induction was at time zero. (C) Normalized fEPSP amplitudes: The absolute fEPSP amplitudes were normalized to the mean of the 60 baseline recordings before time zero and expressed as percentage of potentiation. The mean of the baseline recordings was set to zero % potentiation. (D) Means of the fEPSP from a hippocampal slice of a neurotrypsin-overexpressing mouse: The fiber volley, which is somewhat larger here than in the control experiment, can be discerned easily. The dashed line in the second trace represents the baseline trace. (E) Recording of the fEPSP amplitudes from a hippocampal slice of a neurotrypsin-overexpressing mouse. F: Normalized fEPSP amplitudes. In this hippocampal slice of the neurotrypsin-overexpressing mouse (DTG), the fEPSP reached and maintained a higher percentage of potentiation than in the slice of the control mouse.

Fig. 11
Mean potentiation of the pooled and normalized fEPSP experiments concerning LTP. Each point represents the mean peak amplitude calculated from the pooled slopes of the fEPSP experiments. Compared are the results from animals belonging to the control and the neurotrypsin-overexpressing group (DTG). The fEPSP time courses are normalized to the mean of the base-line responses and expressed as percentage of potentiation. The dashed line represents potentiation of zero %. The error bars represent the standard deviation of this average. For clarity of presentation, error bars are shown in one direction only, pointing upwards for the group of neurotrypsin-overexpressing mice (DTG) and downwards for the control group (control). The dots above the graph indicate where the difference between the

means of the two groups reaches significance (p 0.05, determined by a paired Student t test).

Fig. 12
Demonstration of the reverberating activity observed in the hippocampus of neurotrypsin-overexpressing mice. (A) Means from fEPSP traces from a slice of a neurotrypsin-overexpressing mouse. a) The trace was obtained from 60 baseline recordings. b) The trace was obtained from 240 recordings after induction of LTP. (B) Means from fEPSP traces from a control slice a) The trace was obtained from 60 baseline recordings. b) The trace was obtained from 240 recordings after induction of LTP. The dashed lines in Ab and Bb represent the previous trace, taken from Aa and Ba, respectively.

Fig. 13
Charging curve of pyramidal cells in the CA1 region of the hippocampus. A current clamped at 0.03 nA was injected 0.3 seconds in the soma of pyramidal CA1 cells of the hippocampus through the patch pipette and the resultant change in the membrane potential was measured during 0.3 seconds. Displayed by the dashed lines is the 63% level of the maximum voltage change and the corresponding time.

Fig. 14
Reconstructed CA1 pyramidal cells. The left cell is from a hippocampal slice of a wild-type mouse, the right from a hippocampal slice of a neurotrypsin-overexpressing (DTG) mouse. The cells shown were randomly selected; the differences between them do not indicate a size difference in the dendrites of neurons of neurotrypsin-overexpressing and wild-type mice (for quantitative data see Fig. 15). Scale bar, 100 µm.

Fig. 15
Comparison of the spatial properties of reconstructed CA1 pyramidal cells. No significant difference was detected in any of the measurements. (White bars: control mice, n = 8, black bars: neurotrypsin-overexpressing mice, n = 11).

Fig. 16
Electron microscopic comparison of synapses of the hippocampal stratum radiatum of wild-type and neurotrypsin-overexpressing mice. Synapses of neurotrypsin-overexpressing mice are smaller than synapses of wild-type mice (for a quantification see Fig. 17 – 20). Note also the relatively small number of synaptic vesicles in the presynaptic axon terminals of neurotrypsin-overexpressing mice (arrows).

Fig. 17
Quantification of the number of synapses per volume of tissue in the neuropil of the stratum radiatum of the CA1 region of the hippocampus. In all experimental animals, the number of synapses per volume of tissue was determined from electron microscopic sections taken from the same location in the stratum radiatum of the CA1 region of the hippocampus. wt: wild type; CMV-Cre: transgenic line expressing the Cre recombinase under the control of the CMV promoter; 491(inact.Nt): transgenic line 491, bearing the inactive transgene, containing a transcriptional stop segment; 494(inact.Nt): transgenic line 494, bearing the inactive transgene, containing a transcriptional stop segment; DTG(Nt491/cre): double transgenic mouse descending from the line 491, in which the inactive neurotrypsin transgene has been activated by crossing in the Cre recombinase; DTG(Nt494/cre): double transgenic mouse descending from the line 494, in which the inactive neurotrypsin transgene has been activated by crossing in the Cre recombinase. (**, $p < 0.01$).

Fig. 18
Quantification of the axon terminal area in the neuropil of the stratum radiatum of the CA1 region of the hippocampus. In all experimental animals, the axon terminal area of axons that

form asymmetric synapses was determined from electron microscopic sections taken from the same location in the stratum radiatum of the CA1 region of the hippocampus. wt: wild type; CMV-Cre: transgenic line expressing the Cre recombinase under the control of the CMV promoter; 491(inact.Nt): transgenic line 491, bearing the inactive transgene, containing a transcriptional stop segment; 494(inact.Nt): transgenic line 494, bearing the inactive transgene, containing a transcriptional stop segment; DTG(Nt491/cre): double transgenic mouse descending from the line 491, in which the inactive neurotrypsin transgene has been activated by crossing in the Cre recombinase; DTG(Nt494/cre): double transgenic mouse descending from the line 494, in which the inactive neurotrypsin transgene has been activated by crossing in the Cre recombinase. (*, $p < 0.05$; **, $p < 0.01$).

Fig. 19
Quantification of the synaptic lengths of axospinous synapses in the neuropil of the stratum radiatum of the CA1 region of the hippocampus. In all experimental animals, the number of synapses per volume of tissue was determined from electron microscopic sections taken from the same location in the stratum radiatum of the CA1 region of the hippocampus. As a measure of the synaptic length, the length of the parallel alignment of the presynaptic and the postsynaptic membrane enclosing the synaptic cleft was measured. wt: wild type; CMV-Cre: transgenic line expressing the Cre recombinase under the control of the CMV promoter; 491(inact.Nt): transgenic line 491, bearing the inactive transgene, containing a transcriptional stop segment; 494(inact.Nt): transgenic line 494, bearing the inactive transgene, containing a transcriptional stop segment; DTG(Nt491/cre): double transgenic mouse descending from the line 491, in which the inactive neurotrypsin transgene has been activated by crossing in the Cre recombinase; DTG(Nt494/cre): double transgenic mouse descending from the line 494, in which the inactive neurotrypsin transgene has been activated by crossing in the Cre recombinase. (*, $p < 0.05$).

Fig. 20
Quantification of the cross-sectional area of dendritic spines in the neuropil of the stratum radiatum of the CA1 region of the hippocampus. In all experimental animals, the postsynaptic dendritic spines that form synapses were determined from electron microscopic sections taken from the same location in the stratum radiatum of the CA1 region of the hippocampus. wt: wild type; CMV-Cre: transgenic line expressing the Cre recombinase under the control of the CMV promoter; 491(inact.Nt): transgenic line 491, bearing the inactive transgene, containing a transcriptional stop segment; 494(inact.Nt): transgenic line 494, bearing the inactive transgene, containing a transcriptional stop segment; DTG(Nt491/cre): double transgenic mouse descending from the line 491, in which the inactive neurotrypsin transgene has been activated by crossing in the Cre recombinase; DTG(Nt494/cre): double transgenic mouse descending from the line 494, in which the inactive neurotrypsin transgene has been activated by crossing in the Cre recombinase. (*, $p < 0.05$).

Fig. 21
Spines on secondary dendritic branches of CA1 pyramidal neurons of wild-type mice (A and B) and double-transgenic mice overexpressing neurotrypsin (C and D). CA1 pyramidal cells were iontophoretically filled with biocytin during electrophysiological in vitro studies and visualised using avidin-biotin-peroxidase histochemistry. Dendrites of wild-type mice have many long, well-developed spines (large arrows); in addition, many short, stubby-shape spines (small arrowheads) are also found. Dendrites of neurotrypsin-overexpressing mice (littermates) are dominated by short stubby-shape spines (small arrowheads); long, well-developed spines (large arrows) are very rare. Note, also, that the total spine density (number of spines per unit length of dendrite) is markedly lower in neurotrypsin-overexpressing mice (C and D).

Fig. 22
Immunofluorescent detection of agrin and neurotrypsin in transiently transfected HEK293T cells. Semi-confluent HEK293T cells on glass coverslips in 3 ml DMEM/10% FCS in a 3 cm well were transiently transfected with 5 μg of either pcDNA3.1-neurotrypsin, or pcDNA3.1-agrin, or both, respectively, using Ca-phosphate precipitation. 48 hrs after transfection the cells were washed, fixed with 4 % paraformaldehyde and processed for indirect immunofluorescence with rabbit polyclonal anti-neurotrypsin antiserum (SZ177, 1:300; Texas red-conjugated secondary anti-rabbit IgG antibody; A,C,E,G,I) and monoclonal anti-agrin antibody (AGR540, Stressgen, 1:600; FITC-conjugated secondary anti-mouse IgG antibody; B,D,F,H,K). Single transfections of non-permeabilized cells are shown in (A,B). Double transfections of non-permeabilized cells are shown in (C,D). Cell surface agrin immunoreactivity is absent in the presence of neurotrypsin (D). Double transfections of permeabilized cells are shown in (E,F). Agrin immunoreactivity is present intracellularly (F). Double transfections with catalytically inactive neurotrypsin and agrin are shown with non-permeabilized (G,H) and permeabilized cells (I,K). Agrin immunoreactivity remains at the cell surface in the presence of catalytically inactive neurotrypsin (H). Note the clear membrane accumulation of neurotrypsin in the presence of agrin (C,E,G,I), but not in the absence (A). Digital images were taken on a Leica microscope at 630x magnification and processed with Adobe Photoshop and Microsoft PowerPoint.

Fig. 23
Western blot analysis of agrin from transiently transfected HEK293 cells. Semi-confluent HEK293T cells in 2 ml DMEM/10% FCS in a 3 cm well were transiently transfected with 5 μg of either pcDNA3.1-neurotrypsin, or pcDNA3.1-agrin, or both, respectively, using Ca-phosphate precipitation. 48 hrs after transfection the medium was removed, proteins were precipitated and redissolved in Laemmli loading buffer. The cells were washed with PBS. A 1 % Triton X-100 detergent extract was prepared. Samples from the extract (30 μg, equivalent to 1/8 of totally extracted protein) and concentrated media were separated by SDS-PAGE and transferred to nitrocellulose. Cell extracts of agrin- (lane 1), agrin plus neurotrypsin- (lane 2), and control-transfected (lane 3) assays were probed with the polyclonal anti-agrin antibody K-17 (Santa Cruz; 1:1,000). 200 μl medium from such an experiment, and additionally from a double transfection with agrin and catalytically inactive neurotrypsin (NT(S/A)), were tested with the monoclonal anti-agrin antibody AGR540 (Stressgen; 1:1,000; lanes 4-6). In lanes 7 and 8, 100 μl and 50 μl of medium from an agrin/neurotrypsin double transfection were loaded, respectively. For detection of the primary antibodies, HRP-coupled secondary antibodies were used. HRP activity was visualized by chemiluminescence. A soluble 100-kDa agrin fragment is produced in the presence of neurotrypsin. Positions of molecular mass markers are indicated at the left margin (in kDa).

Fig. 24
Domain structure of neurotrypsin. (A) Neurotrypsin of the mouse. (B) Human Neurotrypsin. Human neurotrypsin is composed of a proline-rich basic domain (PB), a kringle domain, four scavenger receptor cysteine-rich domains (SRCR1, SRCR2, SRCR3, and SRCR4), and a protease domain (PROT). In neurotrypsin of the mouse, only 3 SRCR domains are found. The zymogen activation site (ZA) represents a potential cleavage site at the N-terminus of the protease domain of neurotrypsin. Proteolytic cleavage at the ZA site converts the neurotrypsin protein from a catalytically inactive to a catalytically active form. By this cleavage, a fragment of approximately 55 kDa, comprising the non-catalytic region, and a fragment of approximately 30 kDa, comprising the protease domain, are generated in the case of mouse neurotrypsin. In the case of human neurotrypsin, the fragments generated have 67 kDa and 30 kDa, respectively. The putative disulfide bond connecting the protease domain with the third SRCR domain is indicated (S-S). Asterisks indicate potential N-glycosylation sites.

Fig. 25
Expression of recombinant neurotrypsin in HEK293T cells. Ten μg total protein of each fraction was separated on a 10% SDS PAGE and then transferred to a nitrocellulose membrane. Recombinant protein was detected with an anti-Tetra-His antibody (QIAGEN, dilution 1:2000) and a goat-anti-mouse secondary antibody coupled to peroxidase(KPL, dilution 1:7500) followed by detection with ECL reagent (Amersham Pharmacia Biotech). ST: molecular weight marker (kDa); +: cells transfected with pcDNA3.1 coding for mouse neurotrypsin; -: cells transfected with empty pcDNA3.1 (control). The arrow indicates the band of 85 kDa representing neurotrypsin.

Fig. 26
Expression of neurotrypsin in HEK293-EBNA cells. HEK293T and HEK293-EBNA cells were transiently transfected with either pcDNA3.1-neurotrypsin (control) or pEAK8-neurotrypsin, respectively. - negative control, transfection with empty pcDNA3.1 or empty pEAK8. Ten μg of total cell extracts from transfected HEK293T and HEK293-EBNA cells were loaded and separated on a 10% SDS PAGE (upper panel). In addition, media supernatant was loaded using equal volume (lower panel). Proteins were transferred to a nitrocellulose membrane. Detection of neurotrypsin was performed with the neurotrypsin-specific antibody SZ177 binding to the basic proline-rich domain (dilution 1:3,000) and a secondary goat-anti-rabbit antibody coupled to peroxidase (Sigma; dilution 1:2,000). Control: HEK293T; ST: molecular weight marker (kDa). P1 to P4 represent different transfection experiment with varying amounts of DNA transfected (P1: 200 μg, P2: 150 μg, P3: 75 μg and P4: 50 μg. f.l.NT, full-length neurotrypsin; cl.NT, cleaved neurotrypsin (here detected is the band of approximately 55 kDa corresponding to the non-catalytic fragment).

Fig. 27
Expression of neurotrypsin in High 5 insect cells. High 5 insect cells were infected with recombinant baculovirus at an MOI of 4. Supernatants were harvested 3 days post-infection and separated on a 10% SDS PAGE. After transferring the proteins on a nitrocellulose membrane, neurotrypsin was detected with the neurotrypsin-specific antibody SZ177 (dilution 1:3000) and a goat-anti-rabbit antibody coupled to peroxidase detecting the full-length protein and the non-catalytic fragment (A and B) under reducing conditions. The full-length form of neurotrypsin and the protease domain were detected using the G73 antibody binding to the protease domain and the secondary antibody rabbit-anti-goat coupled with peroxidase (dilution 1:20000). In addition, neurotrypsin conformation was analysed under reducing and non-reducing conditions (B). Detection was performed with the SZ177 antibody. ST, molecular weight marker (kDa); f.l.NT, full-length neurotrypsin; cl.NTnterm, non-catalytic fragment; f.l.NTcl., full-length and cleaved form under non-reducing conditions; c.l.NTprot., protease domain of cleaved neurotrypsin.

Fig. 28
Expression of neurotrypsin in J558L mouse myeloma cells. Stable clones expressing neurotrypsin were generated by protoplast fusion. Cell extracts and supernatants were collected and separated on a 10% SDS PAGE. Proteins were transferred to a nitrocellulose membrane. Detection of neurotrypsin was performed with either the neurotrypsin-specific antibody SZ177 binding the basic proline-rich domain (dilution 1:3000) and a secondary goat-anti-rabbit antibody coupled to peroxidase (Sigma; dilution 1:20000) or G73 binding the protease domain (dilution 1:500) and a rabbit-anti-goat antibody coupled to peroxidase (dilution 1:20000). 1 and 2 represent two different clones analysed. S, supernatant; CE, cell extract; molecular weight marker in kDa; f.l.NT, full-length neurotrypsin; cl.NTnterm, non-catalytic fragment of cleaved neurotrypsin; cl.NTprot, protease domain of cleaved neurotrypsin.